

# A Joint Power Splitting, Active and Passive Beamforming Optimization Framework for IRS Assisted MIMO SWIPT System

Chen He, *Member, IEEE*, Xie Xie, Kun Yang, *Senior Member, IEEE*, and Z. Jane Wang, *Fellow, IEEE*

**Abstract**—This paper considers an intelligent reflecting surface (IRS) assisted multi-input multi-output (MIMO) power splitting (PS) based simultaneous wireless information and power transfer (SWIPT) system with multiple PS receivers (PSRs). The objective is to maximize the achievable data rate of the system by jointly optimizing the PS ratios at the PSRs, the active transmit beamforming (ATB) at the access point (AP), and the passive reflective beamforming (PRB) at the IRS, while the constraints on maximum transmission power at the AP, the reflective phase shift of each element at the IRS, the individual minimum harvested energy requirement of each PSR, and the domain of PS ratio of each PSR are all satisfied. For this unsolved problem, however, since the optimization variables are intricately coupled and the constraints are conflicting, the formulated problem is non-convex, and cannot be addressed by employing exist approaches directly. To this end, we propose a joint optimization framework to solve this problem. Particularly, we reformulate it as an equivalent form by employing the Lagrangian dual transform and the fractional programming transform, and decompose the transformed problem into several sub-problems. Then, we propose an alternate optimization algorithm by capitalizing on the dual sub-gradient method, the successive convex approximation method, and the penalty-based majorization-minimization approach, to solve the sub-problems iteratively, and obtain the optimal solutions in nearly closed-forms. Numerical simulation results verify the effectiveness of the IRS in SWIPT system and indicate that the proposed algorithm offers a substantial performance gain.

**Index Terms**—Intelligent reflecting surface, Simultaneous wireless information and power transfer, Power splitting, Joint optimization, Lagrangian dual transform.

## I. INTRODUCTION

Radio frequency (RF) signals can transfer both information and energy simultaneously, which makes it possible to combine wireless power transfer (WPT) and wireless information transfer (WIT) [1]. Motivated by this fact, currently, simultaneous wireless information and power transfer (SWIPT) [2] has been regarded as an appealing technology for the internet of things (IOT) with low-power and energy-limited devices [3]. However, SWIPT also brings new challenges on the trade-off of information decoding (ID) and energy harvesting (EH) operations, which needs to be addressed in the SWIPT system

[4]–[6]. In SWIPT system ID receivers and EH receivers can be separated or integrated [7], [8]. For the separated architecture, the ID receivers and the EH receivers are different devices. The former is only able to process information and the latter is only for power charging. In contrast, for the integrated architecture, each receiver has integrated circuitry to perform both ID and EH operations, by power splitting (PS) [9] or time switching (TS). In particular, PS receivers (PSRs) split the received signal into two streams of different power, one for ID operation and the other for EH, and TS receivers (TSRs) split the received signal in time domain.

Compared with the conventional receivers, the receivers in SWIPT is more limited by the received energy strength, as a portion of the power must be used to active the circuit. This leads to a performance bottleneck in SWIPT system. MIMO technology can significantly improve the performance of the SWIPT systems by providing increased link capacity and spectral efficiency [10], [11]. Employing relays is another way to enhance the performance of the SWIPT systems, which can introduce additional links to strengthen the received signal power at the receivers.

Remarkably, there is another promising and cost-effective technique, namely intelligent reflecting surface (IRS), to improve the spectral and energy efficiency of wireless communications systems, due to the fact that IRS can introduce several reflective channels to mitigate detrimental propagation environment. In general, an IRS can adjust the wireless propagation environment nearly-instantaneously, by using a vast number of nearly-passive reflective elements, each of which can change the phase of the signals without introducing additional noise [12]–[15]. Optimal PRB design [16]–[18], which can maximize the achievable data rate, is the major challenge for the IRS-assisted communications systems. The work [19] considered a two-way communications with the IRS and maximized the data rate by employing the Arimoto-Blahut algorithm. The authors in [20] studied the sum-rate maximization problem under MISO setting and proposed an efficient algorithm based on the vector versions of Lagrangian dual transform (LDT) and fractional programming transform (FPT) [21]–[23]. The work [24] employed the same vector versions of LDT and FPT as those in [20] to solve this sum-rate maximization problem in the more general and complex cell-free scenario. In [25], by proposing an majorization-minimization (MM) based [26] algorithm, the authors maximized the sum-rate of all groups for an IRS-assisted multi-group multi-cast communications system. Moreover, the au-

Chen He and Xie Xie are with the School of Information Science and Technology, Northwest University, Xi'an, 710069, China. Corresponding author: Chen He (email: chenhe@nwu.edu.cn).

Kun Yang is with the School of Information Science and Technology, Northwest University, Xi'an, 710069, China, and he is also with School of Computer Science & Electronic Engineering, University of Essex, Wivenhoe Park, Colchester, Essex CO4 3SQ, United Kingdom.

Z. Jane Wang is with Department of Electrical and Computer Engineering, The University of British Columbia, Vancouver, BC V6T1Z4, Canada.

thors in [27] and [28] considered the sum-rate maximization problem in multi-cell multi-IRS scenario. Particularly, the authors in [27] employed the well-known weighted minimum mean-square error (WMMSE) [29] technique to transform the original sum-rate maximization problem into an equivalent form, and solved it based on the block coordinate descent (BCD) technique, the Lagrangian multiplier method and the Complex Circle Manifold (CCM)/MM algorithms. The authors in [28] proposed an algorithm based on the second-order cone programming (SOCP) and semi-definite relaxation (SDR) [30] techniques. Furthermore, other wide ranges of topics in IRS-assisted communications system had also been studied, such as power allocation, physical layer security, non-orthogonal multiple access, device-to-device communication, and so on [31]–[35].

Recently, deploying the IRS into the SWIPT system has been attracting increasing attentions. The authors in [36] considered deploying IRS to enhance the physical layer security in SWIPT system. The authors in [37] proposed an efficient penalty-based algorithm developed through SCA and SDR approaches to optimize resource allocations in an IRS-assisted SWIPT system, in which a dedicated energy-carrying signal was required, and the EH receiver model was non-linear. Meanwhile, the authors in [38] proved the dedicated energy signal can only slightly improve the performance, and provided a SDR-based algorithm. Moreover, the authors in [39] investigated a transmission power minimization problem under quality-of-services (QoS) constraints, and proposed a penalty-based optimization method to solve it. The achievable data rate maximization problem with separated ID and EH receivers was investigated in [40], in which the authors transformed the data rate maximization problem as an equivalent WMMSE minimization problem by exploiting the equivalence between the data rate and WMMSE, and proposed an efficient iterative algorithm based on BCD and MM technologies. The paper [41] studied an IRS-aided SWIPT system with multiple integrated PSRs, and introduced an energy efficiency indicator (EEI) to balance the data rate and harvested energy. Then an efficient algorithm developed by SDR technique, MM algorithm and Dinkelbach approach, was proposed for addressing this problem. In [42], the authors studied the maximum energy efficiency of the IRS-assisted SWIPT system, and proposed an efficient alternate optimization (AO) algorithm by capitalizing on the penalty-based method, SDR technique and MM approach.

Most exiting works on IRS-assisted MIMO SWIPT systems focus on minimizing the transmission power, or maximizing the received power, or maximizing energy efficiency [36]–[39], [41], [42]. For the work on IRS-assisted MIMO SWIPT system focusing on maximizing sum-rate, the receivers for ID and EH are separated devices [40]. In this paper, however, we consider the achievable data rate maximization problem in the IRS-assisted MIMO SWIPT system with multiple integrated PSRs, in which the receivers can perform both ID and EH. To our best knowledge, this problem has not been addressed yet, and is fundamentally different from the above mentioned problems in IRS-assisted SWIPT systems. As we will see later, the optimization problem investigated in this paper is non-convex

since the optimization variables are intricately coupled, and the constraints are conflicting, which impose a big challenge for solving the problem.

The main contributions of this paper are summarized as follows

- In order to solve this non-convex and challenging optimization problem, we propose a joint optimization framework. Particularly, we employ the matrix versions of LDT and FPT, to transform the problem into an equivalent form, in which the optimization variables are decoupled. Given the fact that the objective function of transformed problem with respect to each variable is concave with the others being fixed, consequently, we decompose the transformed problem into several sub-problems. Then, we propose an AO-based algorithm to solve this sub-problems and obtain the solutions of all variables in nearly closed-forms. We also prove that the finally solutions satisfy the Karush-Kuhn-Tucker (KKT) conditions of the original problem;
- At the PSRs side, we design of the optimal PSRs, i.e., the optimal PS ratios for the EH and ID operations, and the optimal decoding filters (matrices) for decoding the received signals. It is worth to mention here that when optimizing the PS ratio of each PSR for the EH and ID operations, each iteration will yield an upper bound of PS ratios, which can be used to check the feasibility of the problem;
- At the AP side, first, by approximating minimum harvested energy requirement, which is a non-convex constraint, to a linear form, we reformulate the optimization sub-problem of ATB as a convex form. Then we provide a nearly closed-form solution of ATB by exploiting Lagrangian dual sub-gradient method and also prove that the final converged solution of ATB satisfies the KKT conditions of the original sub-problem;
- At the IRS side, we approximate the constraint of minimum harvested energy by adopting SCA approach and then transform the optimization sub-problem of PRB as a quadratic programming (QP) form under constant modulus constraints after further matrix manipulations. Since the constant modulus constraint of each reflective element is non-convex, the QP problem is still non-convex, and the dual gap is not guaranteed to be zero. To solve this problem with low-complexity, we propose an efficient penalty-based MM algorithm and obtain the solution of PRB in a nearly closed-form. It can also be readily verified that the final converged solution satisfies the KKT conditions of the original sub-problem of optimizing PRB;
- Finally, simulation results indicate that the IRS can provide a significant performance gain, and the proposed algorithm can substantially enhance the performance.

*Notations:* Boldface low case letters denote vectors and upper case letters stand for matrices.  $\mathbb{C}^{M \times N}$  represents a complex matrix with the dimensional of  $M \times N$ .  $\mathbf{I}_N$  and  $\mathbf{0}$  denote the  $N \times N$  identity matrix and zero matrix. For two matrices  $\mathbf{A}$  and  $\mathbf{B}$ ,  $\mathbf{A} \odot \mathbf{B}$  and  $\mathbf{A} \otimes \mathbf{B}$  are the Hadamard product

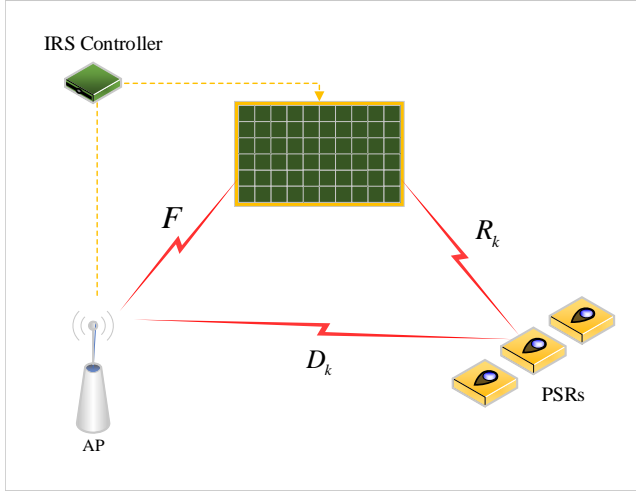


Fig. 1. IRS-assisted PS-SWIPT System.

and Kronecker product of  $\mathbf{A}$  and  $\mathbf{B}$ , respectively. For a square matrix  $\mathbf{A}$ ,  $\mathbf{A}^H$ ,  $\mathbf{A}^T$  and  $\text{Tr}(\mathbf{A})$  denote the Hermitian conjugate transpose, the transpose, and the trace of matrix  $\mathbf{A}$ , respectively.  $\text{diag}(\cdot)$  denotes the diagonal operation and  $\Re\{\cdot\}$  denotes the real part of a complex number. Meanwhile,  $\mathcal{O}$  denotes the computational complexity notation.

## II. SYSTEM MODEL AND PROBLEM FORMULATION

In this section, as shown in Fig. 1, we describe an IRS-assisted SWIPT system with multiple integrated PSRs. Meanwhile, it is assumed that the AP and the IRS controller can acquire the channel state information (CSI) perfectly [43].<sup>1</sup> We define  $M_b$  and  $M_u$  as the number of the AP antennas and the PSRs antennas, respectively. Meanwhile,  $N$  denotes the number of reflective elements of the IRS.

The signal at the AP,  $\mathbf{x}$ , is a combination of symbols intended to  $K$  PSRs, which is given as  $\mathbf{x} = \sum_{k=1}^K \mathbf{W}_k \mathbf{s}_k$ , where  $\mathbf{s}_k \in \mathbb{C}^{M_u \times 1}$  is the data symbol vector, and satisfies  $\mathcal{CN}(\mathbf{0}, \mathbf{I}_{M_u})$ , and  $\mathbf{W}_k \in \mathbb{C}^{M_b \times M_u}$  denotes the corresponding ATB matrix for the  $k^{\text{th}}$  PSR.

The received signal at the  $k^{\text{th}}$  PSR can be expressed as

$$\mathbf{y}_k = \mathbf{H}_k^H \mathbf{W}_k \mathbf{s}_k + \sum_{i=1, i \neq k}^K \mathbf{H}_k^H \mathbf{W}_i \mathbf{s}_i + \mathbf{n}_k, \forall k, \quad (1)$$

where  $\mathbf{n}_k \sim \mathcal{CN}(\mathbf{0}, \sigma_k^2 \mathbf{I}_{M_u})$  denotes the antenna noise vector at the  $k^{\text{th}}$  PSR, and  $\mathbf{H}_k \in \mathbb{C}^{M_b \times M_u}$  denotes the cascade channel from the AP to the  $k^{\text{th}}$  PSR, and can be mathematically expressed as  $\mathbf{H}_k = \mathbf{D}_k + \mathbf{R}_k^H \Theta \mathbf{F}$ , where  $\mathbf{D}_k \in \mathbb{C}^{M_b \times M_u}$  denotes the direct channel from the AP to the  $k^{\text{th}}$  PSR,  $\mathbf{R}_k \in \mathbb{C}^{N \times M_u}$  is the channel from the IRS to the  $k^{\text{th}}$  PSR and the channel from the AP to the IRS is represented by  $\mathbf{F} \in \mathbb{C}^{N \times M_b}$ . Since the signals impinging by the IRS and will

<sup>1</sup>The conventional channel estimation methods can directly applied for the IRS and there are others channel estimation technologies designed only for IRS system. However, in fact, the required CSI of IRS channels cannot be accurate, therefore, the robust optimization algorithm need to be proposed [16], which is left for future work.

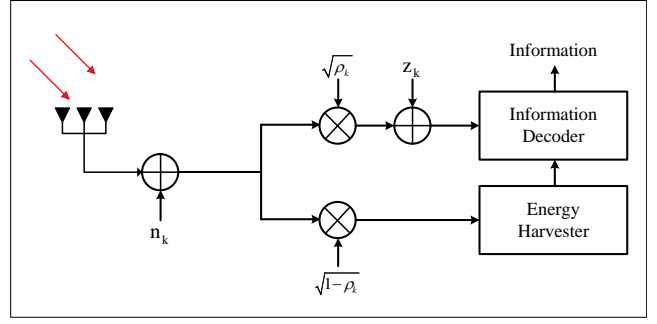


Fig. 2. Architecture of Integrated PSR.

be absorbed, which may lead to a power loss, thus, the PRB of IRS can be represented by

$$\Theta = \alpha \text{diag}(e^{j\phi_1}, e^{j\phi_2}, \dots, e^{j\phi_N}), \quad (2)$$

where  $\phi_n \in [0, 2\pi)$ ,  $\forall n \in N$  is the phase shift of  $n^{\text{th}}$  reflective element, and  $\alpha$  denotes reflecting efficiency of IRS.<sup>2</sup>

In this paper, as shown in Fig. 2, each PSR is an integration of an ID receiver and a EH receiver, and the received signal power is split into two streams by an adjustable PS ratio of  $\rho_k \in (0, 1)$ , which is dedicated for ID operation, and  $1 - \rho_k$  is exploited for EH operation. Accordingly, the received signal power splits for ID operation can be expressed as

$$\mathbf{y}_k^{\text{ID}} = \sqrt{\rho_k} \left( \mathbf{H}_k^H \mathbf{W}_k \mathbf{s}_k + \sum_{i=1, i \neq k}^K \mathbf{H}_k^H \mathbf{W}_i \mathbf{s}_i + \mathbf{n}_k \right) + \mathbf{z}_k, \forall k, \quad (3)$$

where  $\mathbf{z}_k \sim \mathcal{CN}(\mathbf{0}, \delta_k^2 \mathbf{I}_{M_u})$  is the additional noise generated during signal processing. Therefore, the signal to interference plus noise ratio (SINR) at the  $k^{\text{th}}$  PSR can be formulated as

$$\Gamma_k = \frac{\rho_k \mathbf{H}_k^H \mathbf{W}_k \mathbf{W}_k^H \mathbf{H}_k}{\rho_k \sum_{i=1, i \neq k}^K \mathbf{H}_k^H \mathbf{W}_i \mathbf{W}_i^H \mathbf{H}_k + \rho_k \sigma_k^2 \mathbf{I}_{M_u} + \delta_k^2 \mathbf{I}_{M_u}}, \forall k. \quad (4)$$

The received signal power splits for EH operation is given as

$$\mathbf{y}_k^{\text{EH}} = \sqrt{1 - \rho_k} \left( \sum_{i=1}^K \mathbf{H}_k^H \mathbf{W}_i \mathbf{s}_i + \mathbf{n}_k \right), \forall k. \quad (5)$$

By ignoring the antenna noise power [42], i.e.,  $\sigma_k^2$ , since it is negligible, the split power for EH can be expressed as

$$\mathbf{e}_k = \eta_k (1 - \rho_k) \text{Tr} \left( \sum_{i=1}^K \mathbf{H}_k^H \mathbf{W}_i \mathbf{W}_i^H \mathbf{H}_k \right), \forall k, \quad (6)$$

where  $\eta_k \in (0, 1)$  is the energy conversion efficiency for the  $k^{\text{th}}$  PSR.

<sup>2</sup>Some previous works assume a more ideal model of IRS as  $\Theta = \text{diag}(\varphi_1 e^{j\phi_1}, \varphi_2 e^{j\phi_2}, \dots, \varphi_N e^{j\phi_N})$ , where  $\varphi_n$  denotes amplitude of  $n^{\text{th}}$  element of IRS. In this ideal model, IRS can reconfigure the incident signal by changing its amplitude and phase shift. Clearly, the ideal IRS model can offer a higher adaptability to reconfigure the incident signals, however, it may also lead to a higher implementation complexity. The trade-off between performance and implementation complexity is a key problem, which is left for future work.

The achievable data rate of all the PSRs can be expressed as  $\mathcal{R}(\rho, \mathbf{W}, \Theta) = \sum_{k=1}^K \log |\mathbf{I}_{M_u} + \Gamma_k|$ . Accordingly, the achievable data rate maximization problem can be defined as

$$\max_{\rho, \mathbf{W}, \Theta} \mathcal{R}(\rho, \mathbf{W}, \Theta) \quad (7)$$

$$\text{s. t.} \quad \sum_{k=1}^K \|\mathbf{W}_k\|_2^F \leq P_{\max}, \quad (7a)$$

$$\text{Tr} \left( \sum_{i=1}^K \mathbf{H}_k^H \mathbf{W}_i \mathbf{W}_i^H \mathbf{H}_k \right) \geq \frac{\bar{e}_k}{\eta_k (1 - \rho_k)}, \forall k, \quad (7b)$$

$$|\Theta_{n,n}| = \frac{1}{\alpha}, \forall n, \quad (7c)$$

$$0 < \rho_k < 1, \forall k, \quad (7d)$$

where the constraint (7a) limits the maximum transmission power  $P_{\max}$  of the AP, the constraints (7b) are imposed to guarantee the harvested power is larger than minimum EH requirement  $\bar{e}_k, \forall k$ , and the constraint (7d) is the bound of the PS ratio of each PSR, and (7c) represents the constant modulus constraints of reflective elements at the IRS.

It is clear that Problem 7 is non-convex and intractable, due to the fact that all the variables are intricately coupled in a function form of logarithmic, and the minimum EH constraint of each PSR is also non-convex and conflicting with maximum transmission power constraint at the AP. Additionally, the constraints on the PS ratios impose another challenge for the optimization problem. To this end, in the next section, we provide an efficient joint optimization framework to solve the problem.

### III. PROPOSED JOINT OPTIMIZATION FRAMEWORK

First, we move the matrix-ratio terms out of the logarithm in the objective function of Problem 7 by employing the matrix version of LDT, and we have the following proposition

**Proposition 1** (Matrix version of LDT). *By introducing an auxiliary diagonal matrix  $\mathbf{U}_k \in \mathbb{C}^{M_u \times M_u}, \forall k$ , Problem 7 can be reformulated as an equivalent form*

$$\max_{\rho, \mathbf{W}, \Theta, \mathbf{U}} f_1(\rho, \mathbf{W}, \Theta, \mathbf{U}) \quad (8)$$

$$\text{s. t.} \quad (7a) - (7d),$$

where the new objective function can be written as

$$f_1(\rho, \mathbf{W}, \Theta, \mathbf{U}) = \sum_{k=1}^K (\log |\mathbf{I}_{M_u} + \mathbf{U}_k| - \text{Tr}(\mathbf{U}_k))$$

$$+ \sum_{k=1}^K \text{Tr}((\mathbf{I}_{M_u} + \mathbf{U}_k) f_2(\rho, \mathbf{W}, \Theta)), \quad (9)$$

where  $f_2(\rho, \mathbf{W}, \Theta)$  is given by

$$f_2(\rho, \mathbf{W}, \Theta) = \mathbf{H}_k^H \mathbf{W}_k \mathbf{V}_k^{-1} \mathbf{W}_k^H \mathbf{H}_k, \quad (10)$$

with  $\mathbf{V}_k = \sum_{i=1}^K \mathbf{H}_k^H \mathbf{W}_i \mathbf{W}_i^H \mathbf{H}_k + \sigma_k^2 \mathbf{I}_{M_u} + \delta_k^2 / \rho_k \mathbf{I}_{M_u}, \forall k$ .

*Proof.* The proposition is the matrix version of LDT, and the detailed proof of this reformulation method is similar to the vector version [21]–[23].  $\square$

Although, the matrix-ratio term, i.e., SINR, has been moved out of the logarithm function, and the transformed problem has been considerably simplified, the transformed problem is still non-convex and difficult to be handled directly since the optimization variables are still coupled in the matrix-ratio term. Hence, we reformulate the transformed problem as the linear form as follows.

**Proposition 2** (Matrix version of FPT). *By introducing auxiliary diagonal matrix  $\mathbf{L}_k \in \mathbb{C}^{M_u \times M_u}, \forall k$ , the above sub-problem can be equivalently transformed to*

$$\max_{\mathbf{W}, \mathbf{L}} f_3(\rho, \mathbf{W}, \Theta, \mathbf{U}, \mathbf{L}) \quad (11)$$

$$\text{s. t.} \quad (7a) - (7d),$$

where  $f_3(\rho, \mathbf{W}, \Theta, \mathbf{U}, \mathbf{L})$  can be expressed as

$$f_3(\rho, \mathbf{W}, \Theta, \mathbf{U}, \mathbf{L}) = \sum_{k=1}^K \log |\bar{\mathbf{U}}_k| - \sum_{k=1}^K \text{Tr}(\mathbf{U}_k)$$

$$+ \sum_{k=1}^K \text{Tr}(\bar{\mathbf{U}}_k \mathbf{H}_k^H \mathbf{W}_k \mathbf{L}_k^H) + \sum_{k=1}^K \text{Tr}(\bar{\mathbf{U}}_k \mathbf{L}_k \mathbf{W}_k^H \mathbf{H}_k)$$

$$- \sum_{k=1}^K \text{Tr} \left( \bar{\mathbf{U}}_k \mathbf{L}_k \sum_{i=1}^K \mathbf{H}_k^H \mathbf{W}_i \mathbf{W}_i^H \mathbf{H}_k \mathbf{L}_k^H \right)$$

$$- \sum_{k=1}^K \text{Tr}(\bar{\mathbf{U}}_k \mathbf{L}_k (\sigma_k^2 \mathbf{I}_{M_u} + \delta_k^2 / \rho_k \mathbf{I}_{M_u}) \mathbf{L}_k^H), \quad (12)$$

where  $\bar{\mathbf{U}}_k \triangleq \mathbf{U}_k + \mathbf{I}_{M_u}, \forall k$ .

*Proof.* The proposition is extend FPT from the vector into the matrix version, the details proof please refer to [21]–[23].  $\square$

Note that the optimization variables in Problem 11 are decoupled, and the objective function in (12) of Problem 11 is concave with respect to any one of  $\rho, \mathbf{W}, \Theta, \mathbf{U}$  and  $\mathbf{L}$ , with the others being fixed. Based on this fact, we decompose Problem 11 into several sub-problems, and solve them alternately at three sides, i.e., the PSRs side, the AP side and the IRS side. In the  $t$ -th iteration, we have

#### A. Optimization at the PSRs side

Clearly, to design the optimal PSRs, we need to optimize three variables related to the PSRs, i.e.,  $\mathbf{U}, \rho$  and  $\mathbf{L}$ .

First, we consider to optimize the auxiliary diagonal matrix of  $\mathbf{U}_k, \forall k$ . With fixed  $\rho^{(t)}, \mathbf{W}^{(t)}, \Theta^{(t)}$  and  $\mathbf{L}^{(t)}$ , the solution of  $\mathbf{U}$  can be obtained by solving the following sub-problem

$$\mathbf{U}^{(t+1)} \triangleq \arg \max_{\mathbf{U}} f_3(\rho^{(t)}, \mathbf{W}^{(t)}, \Theta^{(t)}, \mathbf{U}, \mathbf{L}^{(t)}). \quad (13)$$

Note that the variable  $\mathbf{U}$  only appears in the objective function of the Sub-problem 13 and does not exist in any constraint set. Therefore, by setting the partial derivatives of the objective function in Sub-problem 13 with respect to  $\mathbf{U}_k, \forall k$  to be zero, and after some matrix manipulations, the closed-form solution is given as

$$\mathbf{U}_k^{(t+1)} = \Gamma_k, \forall k. \quad (14)$$

Note that the variables  $\rho, \mathbf{W}, \Theta$  and  $\mathbf{L}$  only exists in some terms of  $f_3(\mathbf{W}, \Theta, \mathbf{U}, \mathbf{L})$ , with the obtained  $\mathbf{U}^{(t+1)}$  in (14),

we can recast the objective function as  $f_3(\rho, \mathbf{W}, \Theta, \mathbf{U}, \mathbf{L}) \triangleq f_4(\rho, \mathbf{W}, \Theta, \mathbf{L}) + \text{Const}(\mathbf{U})$ , where

$$\begin{aligned} f_4(\rho, \mathbf{W}, \Theta, \mathbf{L}) &= \sum_{k=1}^K \text{Tr}(\bar{\mathbf{U}}_k \mathbf{H}_k^H \mathbf{W}_k \mathbf{L}_k^H) \\ &+ \sum_{k=1}^K \text{Tr}(\bar{\mathbf{U}}_k \mathbf{L}_k \mathbf{W}_k^H \mathbf{H}_k) \\ &- \sum_{k=1}^K \text{Tr}\left(\bar{\mathbf{U}}_k \mathbf{L}_k \sum_{i=1}^K \mathbf{H}_k^H \mathbf{W}_i \mathbf{W}_i^H \mathbf{H}_k \mathbf{L}_k^H\right) \\ &- \sum_{k=1}^K \text{Tr}(\bar{\mathbf{U}}_k \mathbf{L}_k (\sigma_k^2 \mathbf{I}_{M_u} + \delta_k^2 / \rho_k \mathbf{I}_{M_u}) \mathbf{L}_k^H), \end{aligned} \quad (15)$$

and  $\text{Const}(\mathbf{U}) = \sum_{k=1}^K \log |\bar{\mathbf{U}}_k| - \text{Tr}(\mathbf{U}_k)$ . Therefore by fixing the obtained variable of  $\mathbf{U}_k, \forall k$  in (14), we can optimize other variables by only investigating  $f_4$ .

Particularly, we can design the optimal PS ratios of PSRs and check the feasibility of original problem. With fixed  $\mathbf{W}^{(t)}, \Theta^{(t)}$  and  $\mathbf{L}^{(t)}$ , and the obtained  $\mathbf{U}^{(t+1)}$  in (14), the sub-problem for optimizing  $\rho$  is equivalent to

$$\begin{aligned} \rho^{(t+1)} &\triangleq \arg \max_{\rho} f_4(\rho, \mathbf{W}^{(t)}, \Theta^{(t)}, \mathbf{L}^{(t)}) \\ \text{s. t.} & \quad (7b), (7d), \end{aligned} \quad (16)$$

and we have the following lemma

**Lemma 1.** *The objective function of Problem 16 is concave and monotonous increasing with respect to  $\rho$ .*

*Proof.* The proof is presented in Appendix A-A.  $\square$

According to Lemma 1, and considering (7b), (7d) and the objective function in Problem 16 together,  $\rho_k, \forall k$  is required to satisfy the following condition [44], [45]

$$\rho_k^{(t+1)} = 1 - \frac{\bar{\mathbf{e}}_k}{\eta_k \text{Tr}\left(\sum_{i=1}^K \mathbf{H}_k^H \mathbf{W}_i \mathbf{W}_i^H \mathbf{H}_k\right)}, \forall k, \quad (17)$$

and we have the following lemma

**Lemma 2.** *Problem 16 is feasible when  $\rho_k^{(t+1)} > 0, \forall k$ .*

*Proof.* The proof is presented in Appendix A-B.  $\square$

Now, we optimize the variable  $\mathbf{L}_k, \forall k$  with the fixed variables  $\mathbf{W}^{(t)}$  and  $\Theta^{(t)}$ , and the obtained solutions of  $\mathbf{U}^{(t+1)}$  and  $\rho^{(t+1)}$ , by using (14) and (17), respectively. The sub-problem of optimization for  $\mathbf{L}$  is equivalent to

$$\mathbf{L}^{(t+1)} \triangleq \arg \max_{\mathbf{L}} f_4(\rho^{(t+1)}, \mathbf{W}^{(t)}, \Theta^{(t)}, \mathbf{L}). \quad (18)$$

Similar to the method for solving the sub-problem of  $\mathbf{U}$  in (13), the variable  $\mathbf{L}$  does not exist in the constraint set, hence, by setting the partial derivatives of the objective function of the above sub-problem to be zero, the optimal solution of  $\mathbf{L}$  can be obtained as

$$\mathbf{L}_k^{(t+1)} = \mathbf{V}_k^{-1} \mathbf{H}_k^H \mathbf{W}_k, \forall k. \quad (19)$$

Note that  $\mathbf{L}_k, \forall k$  can be treated as the decoding matrix to decode the received signals at the PSRs side, which leads to the

minimum mean-square error (MMSE). For details information, please refer to Appendix B.

Aforementioned, we complete the optimal design at the PSRs side.

### B. Optimization at the AP side

At the AP side, with fixed  $\Theta^{(t)}$ , and the obtained solutions of variables  $\mathbf{U}^{(t+1)}, \rho^{(t+1)}$  and  $\mathbf{L}^{(t+1)}$ , the optimization sub-problem of ATB is defined as

$$\begin{aligned} \mathbf{W}^{(t+1)} &\triangleq \arg \max_{\mathbf{W}} f_4(\rho^{(t+1)}, \mathbf{W}, \Theta^{(t)}, \mathbf{L}^{(t+1)}) \\ \text{s. t.} & \quad (7a), (7b). \end{aligned} \quad (20)$$

By omitting the irrelevant constant term, i.e.,  $\sum_{k=1}^K \text{Tr}(\bar{\mathbf{U}}_k \mathbf{L}_k (\sigma_k^2 \mathbf{I}_{M_u} + \delta_k^2 / \rho_k \mathbf{I}_{M_u}) \mathbf{L}_k^H)$ , which has no impact on the update of  $\mathbf{W}$ , the above optimization problem can be simplified as

$$\begin{aligned} \min_{\mathbf{W}} \sum_{k=1}^K \text{Tr} \left( \bar{\mathbf{U}}_k \mathbf{L}_k \mathbf{H}_k^H \sum_{j=1}^K \mathbf{W}_j \mathbf{W}_j^H \mathbf{H}_k \mathbf{L}_k^H \right) \\ - \sum_{k=1}^K \text{Tr}(\bar{\mathbf{U}}_k \mathbf{H}_k^H \mathbf{W}_k \mathbf{L}_k^H) - \sum_{k=1}^K \text{Tr}(\bar{\mathbf{U}}_k \mathbf{L}_k \mathbf{W}_k^H \mathbf{H}_k) \end{aligned} \quad (21)$$

s. t. (7a), (7b).

Since the minimum EH constraint (7b) is non-convex, the sub-problem to obtain  $\mathbf{W}$  is still challenging. We can exploit SCA approach to approximate the constraint (7b). First, we rewrite the constraint (7b) as

$$\text{Tr} \left( \sum_{i=1}^K \mathbf{W}_i^H \mathbf{B}_k \mathbf{W}_i \right) \geq \bar{\mathbf{e}}_k / \eta_k (1 - \rho_k) \triangleq \dot{\mathbf{e}}_k, \forall k, \quad (22)$$

where  $\mathbf{B}_k \triangleq \mathbf{H}_k \mathbf{H}_k^H$ . Then, by employing the first-order Taylor expansion, in  $n$ -th sub-iteration for updating  $\mathbf{W}$ , we arrive at

$$\begin{aligned} \text{Tr} \left( \sum_{i=1}^K \mathbf{W}_i^H \mathbf{B}_k \mathbf{W}_i \right) &\geq - \text{Tr} \left( \sum_{i=1}^K (\mathbf{W}_i^{(n)})^H \mathbf{B}_k \mathbf{W}_i^{(n)} \right) \\ &+ 2\Re \left\{ \text{Tr} \left( \sum_{i=1}^K (\mathbf{W}_i^{(n)})^H \mathbf{B}_k \mathbf{W}_i \right) \right\}, \forall k. \end{aligned} \quad (23)$$

where  $\mathbf{W}_k^{(n)}, \forall k$ , denotes the solution obtained from the previous sub-iteration. Hence, we can approximate the constraint (7b) by

$$\begin{aligned} 2\Re \left\{ \text{Tr} \left( \sum_{i=1}^K (\mathbf{W}_i^{(n)})^H \mathbf{B}_k \mathbf{W}_i \right) \right\} \\ \geq \dot{\mathbf{e}}_k + \text{Tr} \left( \sum_{i=1}^K (\mathbf{W}_i^{(n)})^H \mathbf{B}_k \mathbf{W}_i^{(n)} \right) \triangleq \ddot{\mathbf{e}}_k^{(n)}, \forall k. \end{aligned} \quad (24)$$

Similarly, by defining  $\mathbf{A}_k \triangleq \mathbf{H}_k \bar{\mathbf{U}}_k \mathbf{L}_k \mathbf{L}_k^H \mathbf{H}_k^H$  and  $\mathbf{A} \triangleq \sum_{k=1}^K \mathbf{A}_k$ , and  $\mathbf{S}_k \triangleq \mathbf{H}_k \bar{\mathbf{U}}_k \mathbf{L}_k$ , we obtain the following problem, which is equivalent to Problem 21

$$\min_{\mathbf{W}} f_5(\mathbf{W}) \triangleq \sum_{k=1}^K \text{Tr}(\mathbf{W}_k^H \mathbf{A} \mathbf{W}_k) - 2 \sum_{k=1}^K \text{Tr}(\mathbf{W}_k^H \mathbf{S}_k) \quad (25)$$

s. t. (7a), (24).

Since the objective function  $f_5(\mathbf{W})$  and the constraint (7a) are both convex, and the constraint (24) is linear, the problem constitutes a convex optimization problem, which can be solved by standard CVX tools [46] directly. However, CVX is employed in each sub-iteration, and this leads to a high computational complexity. Consequently, since the dual gap is guaranteed to be zero, we give the solution of ATB in a nearly closed-form by exploiting Lagrangian dual sub-gradient method. The corresponding Lagrangian function of Problem 25 can be written as

$$\begin{aligned} \mathcal{L}(\mathbf{W} | \mathbf{W}^{(n)}, \tau, \mu) &\triangleq \sum_{k=1}^K \text{Tr}(\mathbf{W}_k^H \mathbf{A} \mathbf{W}_k) - 2 \sum_{k=1}^K \text{Tr}(\mathbf{W}_k^H \mathbf{S}_k) \\ &+ \tau \left( \sum_{k=1}^K \text{Tr}(\mathbf{W}_k^H \mathbf{W}_k) - P_{\max} \right) \\ &- \sum_{k=1}^K \mu_k \left( 2\Re \left\{ \sum_{i=1}^K \text{Tr} \left( \left( \mathbf{W}_i^{(n)} \right)^H \mathbf{B}_k \mathbf{W}_i \right) \right\} - \check{\mathbf{e}}_k^{(n)} \right), \end{aligned} \quad (26)$$

where  $\tau \geq 0$  and  $\mu_k \geq 0, \forall k$  are the Lagrangian multipliers corresponding to the constraints (7a) and (24), respectively. The KKT conditions are given as following

$$\text{Tr} \left( (\mathbf{A} + \tau \mathbf{I}_{M_b}) \mathbf{W}_k - \mathbf{S}_k - \mu_k \mathbf{B}_k \mathbf{W}_k^{(n)} \right) = 0, \forall k; \quad (27)$$

$$\tau \left( \sum_{k=1}^K \text{Tr}(\mathbf{W}_k^H \mathbf{W}_k) - P_{\max} \right) = 0; \quad (28)$$

$$\mu_k \left( 2\Re \left\{ \sum_{i=1}^K \text{Tr} \left( \left( \mathbf{W}_i^{(n)} \right)^H \mathbf{B}_k \mathbf{W}_i \right) \right\} - \check{\mathbf{e}}_k \right) = 0, \forall k. \quad (29)$$

With fixed Lagrangian multipliers of  $\mu_k^{(n)}$  and  $\tau^{(n)}$  in  $n$ -th sub-iteration, the optimal solution of ATB can be explicitly expressed as

$$\mathbf{W}_k^{(n+1)} = \frac{\mathbf{S}_k + \mu_k^{(n)} \mathbf{B}_k \mathbf{W}_k^{(n)}}{\mathbf{A} + \tau^{(n)} \mathbf{I}_{M_b}}, \forall k \in K. \quad (30)$$

Then, we update Lagrangian multipliers with the optimized  $\mathbf{W}_k^{(n+1)}, \forall k$  by employing (30). Particularly, with fixed  $\tau^{(n)}$ ,

---

### Algorithm 1 SCA-based Algorithm for Optimizing ATB

---

**Input:**  $\mathbf{W}_k^{(t)}, \forall k$ , threshold  $\varepsilon$ .

**Output:** Optimal value of  $\mathbf{W}_k^{(t+1)}, \forall k$

1: **Set**  $\mathbf{W}_k^{(0)} \triangleq \mathbf{W}_k^{(t)}, \forall k$ ;

2: **Calculate**

$$f_5(\mathbf{W}^{(0)}) = \sum_{k=1}^K \text{Tr} \left( \left( \mathbf{W}_i^{(0)} \right)^H \mathbf{A} \mathbf{W}_k^{(0)} - 2 \left( \mathbf{W}_i^{(0)} \right)^H \mathbf{S}_k \right);$$

3: **for**  $n = 1$  to  $2, 3, \dots, n_{\max}$  **do**

4:   **Update**  $\check{\mathbf{e}}_k^{(n)}, \forall k$ , by using (24);

5:   **Update**  $\mathbf{W}_k^{(n+1)}, \forall k$ , by using (30);

6:   **if**  $|f(\mathbf{W}^{(n+1)}) - f(\mathbf{W}^{(n)})|/f(\mathbf{W}^{(n)}) < \varepsilon_1$  **then**

6:     **Break** ;

7:   **end if**

8: **end for**

9:  $\mathbf{W}_k^{(t+1)} \triangleq \mathbf{W}_k^{(\hat{n})}, \forall k$ .

---

and by defining  $\bar{\mathbf{A}} = (\mathbf{A} + \tau^{(n)} \mathbf{I}_{M_b})$ , the optimal solution of  $\mu_k$  in a closed-form can be determined as <sup>3</sup>

$$\mu_k^{(n+1)} = \frac{\check{\mathbf{e}}_k^{(n)} - 2\Re \left\{ \sum_{i=1}^K \text{Tr} \left( \left( \mathbf{W}_i^{(n)} \right)^H \mathbf{B}_k \bar{\mathbf{A}}^{-1} \mathbf{S}_k \right) \right\}}{2 \sum_{i=1}^K \text{Tr} \left( \left( \mathbf{W}_i^{(n)} \right)^H \mathbf{B}_k \bar{\mathbf{A}}^{-1} \mathbf{B}_k^H \mathbf{W}_i^{(n)} \right)}, \forall k. \quad (31)$$

Next, we propose an efficient sub-gradient based method to obtain the multiplier associated to the constraint (7a). Particularly, the multiplier  $\tau^{(n+1)}$  can be updated as following

$$\tau^{(n+1)} = \left[ \tau^{(n)} + v \left( \sum_{k=1}^K \text{Tr}(\mathbf{W}_k^H \mathbf{W}_k) - P_{\max} \right) \right]^+, \quad (32)$$

where  $v$  represents the step size for updating  $\tau$  and  $[a]^+ = \max(0, a)$  guaranties  $\tau^{(n+1)}$  being positive.

The SCA-based algorithm for optimization at the AP side is given in Algorithm 1, the finally solution of ATB by employing Algorithm 1 can be expressed as  $\mathbf{W}_k^{(t+1)} \triangleq \mathbf{W}_k^{(\hat{n})}, \forall k$ , where  $\hat{n}$  denotes the maximum number of sub-iterations when Algorithm 1 converges. Now we have the following Lemma

**Lemma 3.** *The sequence of feasible solutions  $\{\mathbf{W}^{(n)}, n = 1, 2, \dots, \hat{n}\}$  generated by Algorithm 1 are optimal solutions of Problem 25. Meanwhile, the final converged solution of Algorithm 1, i.e.,  $\mathbf{W}^{(\hat{n})}$ , also satisfies the KKT conditions of Problem 21.*

*Proof.* The proof is given in Appendix A-C.  $\square$

### C. Optimization at the IRS side

Finally, we consider the optimization at the IRS side. By fixing the obtained solutions of  $\mathbf{U}^{t+1}, \rho^{t+1}, \mathbf{L}^{t+1}$  and  $\mathbf{W}^{t+1}$ ,

<sup>3</sup>To obtain the optimal value of  $\mu$ , we first need to consider the case of  $\mu_k = 0, \forall k$  [47]. In this case, if  $2\Re \left\{ \sum_{i=1}^K \text{Tr} \left( \left( \mathbf{W}_i^{(n)} \right)^H \mathbf{B}_k \mathbf{W}_i^{(n+1)} \right) \right\} \geq \check{\mathbf{e}}_k^{(n)}$  holds, where  $\mathbf{W}_k^{(n+1)} = (\mathbf{A} + \tau^{(n)} \mathbf{I}_{M_b})^{-1} \mathbf{S}_k$ , the optimal value of  $\mu_k^{(n+1)}$  is zero. Otherwise, the optimal value of  $\mu_k > 0$  can be sequentially determined by employing (31).

the corresponding sub-problem for optimizing the PRB of IRS is given as

$$\begin{aligned} \Theta^{(t+1)} \triangleq \arg \max_{\Theta} f_4 \left( \rho^{(t+1)}, \mathbf{W}^{(t+1)}, \Theta, \mathbf{L}^{(t+1)} \right) \quad (33) \\ \text{s. t.} \quad (7b) - (7c). \end{aligned}$$

By substituting  $\mathbf{H}_k^H = \mathbf{D}_k^H + \mathbf{R}_k^H \Theta \mathbf{F}$  into  $\mathbf{H}_k^H \mathbf{W}_k$  and  $\mathbf{H}_k^H \mathbf{W}_i \mathbf{W}_i^H \mathbf{H}_k$ , and defining  $\hat{\mathbf{W}} \triangleq \sum_{j=1}^K \mathbf{W}_j \mathbf{W}_j^H$ , we have

$$\begin{aligned} \mathbf{H}_k^H \mathbf{W}_k &= \mathbf{D}_k^H \mathbf{W}_k + \mathbf{R}_k^H \Theta \mathbf{F} \mathbf{W}_k, \\ \mathbf{H}_k^H \hat{\mathbf{W}} \mathbf{H}_k &= \mathbf{D}_k^H \hat{\mathbf{W}} \mathbf{D}_k + \mathbf{D}_k^H \hat{\mathbf{W}} \mathbf{F}^H \Theta^H \mathbf{R}_k \\ &\quad + \mathbf{R}_k^H \Theta \mathbf{F} \hat{\mathbf{W}} \mathbf{D}_k + \mathbf{R}_k^H \Theta \mathbf{F} \hat{\mathbf{W}} \mathbf{F}^H \Theta^H \mathbf{R}_k. \quad (34) \end{aligned}$$

Then, by substituting them into Sub-problem 33, and defining  $f_4(\rho^{(t+1)}, \mathbf{W}^{(t+1)}, \Theta, \mathbf{L}^{(t+1)}) \triangleq f_6(\Theta) + \text{Consts}(\Theta)$ , where  $\text{Consts}(\Theta)$  denotes the irrelevant constant terms with respect to  $\Theta$ , i.e.,  $\sum_{k=1}^K \text{Tr}(\bar{\mathbf{U}}_k \mathbf{D}_k^H \mathbf{W}_k \mathbf{L}_k^H)$ ,  $\sum_{k=1}^K \text{Tr}(\bar{\mathbf{U}}_k \mathbf{L}_k \mathbf{W}_k^H \mathbf{D}_k)$ ,  $\sum_{k=1}^K \text{Tr}(\bar{\mathbf{U}}_k \mathbf{L}_k \mathbf{D}_k^H \hat{\mathbf{W}} \mathbf{D}_k \mathbf{L}_k^H)$  and  $\sum_{k=1}^K \text{Tr}(\bar{\mathbf{U}}_k \mathbf{L}_k (\sigma_k^2 \mathbf{I}_{M_u} + \delta_k^2 / \rho_k \mathbf{I}_{M_u}) \mathbf{L}_k^H)$ , which have no impact on the update of  $\Theta$ , and where  $f_6(\Theta)$  can be simplified shown as follows

$$\begin{aligned} f_6(\Theta) &= \sum_{k=1}^K \text{Tr}(\bar{\mathbf{U}}_k \mathbf{R}_k^H \Theta \mathbf{F} \mathbf{W}_k \mathbf{L}_k^H) \\ &\quad + \sum_{k=1}^K \text{Tr}(\bar{\mathbf{U}}_k \mathbf{L}_k \mathbf{W}_k^H \mathbf{F}^H \Theta^H \mathbf{R}_k) \\ &\quad - \sum_{k=1}^K \text{Tr}(\bar{\mathbf{U}}_k \mathbf{L}_k \mathbf{D}_k^H \hat{\mathbf{W}} \mathbf{F}^H \Theta^H \mathbf{R}_k \mathbf{L}_k^H) \\ &\quad - \sum_{k=1}^K \text{Tr}(\bar{\mathbf{U}}_k \mathbf{L}_k \mathbf{R}_k^H \Theta \mathbf{F} \hat{\mathbf{W}} \mathbf{D}_k \mathbf{L}_k^H) \\ &\quad - \sum_{k=1}^K \text{Tr}(\bar{\mathbf{U}}_k \mathbf{L}_k \mathbf{R}_k^H \Theta \mathbf{F} \hat{\mathbf{W}} \mathbf{F}^H \Theta^H \mathbf{R}_k \mathbf{L}_k^H). \quad (35) \end{aligned}$$

Consequently, we have the following problem, which is equivalent with Problem 33

$$\begin{aligned} \max_{\Theta} f_6(\Theta) \quad (36) \\ \text{s. t.} \quad (7b) - (7c). \end{aligned}$$

To obtain the solution of  $\Theta$ , we transform Problem 36 to an equivalent QP form under constant modulus constraints. First, by defining  $\mathbf{T}_k = \mathbf{R}_k \mathbf{L}_k^H \bar{\mathbf{U}}_k \mathbf{L}_k \mathbf{R}_k^H$ ,  $\mathbf{Q} = \mathbf{F} \hat{\mathbf{W}} \mathbf{F}^H$ , we have

$$\text{Tr}(\bar{\mathbf{U}}_k \mathbf{L}_k \mathbf{R}_k^H \Theta \mathbf{F} \hat{\mathbf{W}} \mathbf{F}^H \Theta^H \mathbf{R}_k \mathbf{L}_k^H) \triangleq \text{Tr}(\Theta^H \mathbf{T}_k \Theta \mathbf{Q}). \quad (37)$$

Then, by defining  $\mathbf{A}_k = \mathbf{F} \hat{\mathbf{W}} \mathbf{D}_k \mathbf{L}_k^H \bar{\mathbf{U}}_k \mathbf{L}_k \mathbf{R}_k^H$ , we have

$$\text{Tr}(\bar{\mathbf{U}}_k \mathbf{L}_k \mathbf{D}_k^H \hat{\mathbf{W}} \mathbf{F}^H \Theta^H \mathbf{R}_k \mathbf{L}_k^H) \triangleq \text{Tr}(\Theta^H \mathbf{A}_k^H). \quad (38)$$

Next, by defining  $\mathbf{Z}_k = \mathbf{F} \mathbf{W}_k \bar{\mathbf{U}}_k \mathbf{L}_k \mathbf{R}_k^H$ , we have

$$\text{Tr}(\bar{\mathbf{U}}_k \mathbf{R}_k^H \Theta \mathbf{F} \mathbf{W}_k \mathbf{L}_k^H) \triangleq \text{Tr}(\Theta \mathbf{Z}_k). \quad (39)$$

Similar, by defining  $\mathbf{J}_k = \mathbf{R}_k \mathbf{R}_k^H$ ,  $\Lambda_k = \mathbf{F} \hat{\mathbf{W}} \mathbf{D}_k \mathbf{R}_k^H$ , the constraint (7b) can be expressed as

$$\begin{aligned} \text{Tr}(\Theta^H \mathbf{J}_k \Theta \mathbf{Q}) + \text{Tr}(\Theta^H \Lambda_k^H) + \text{Tr}(\Theta \Lambda_k) \\ \geq \hat{\mathbf{e}}_k - \text{Tr}(\mathbf{D}_k^H \hat{\mathbf{W}} \mathbf{D}_k) \triangleq \ddot{\mathbf{e}}_k. \quad (40) \end{aligned}$$

Therefore, by defining  $\mathbf{T} = \sum_{k=1}^K \mathbf{T}_k$ ,  $\mathbf{C} = \sum_{k=1}^K \mathbf{A}_k - \mathbf{Z}_k$ , an equivalent problem is defined as

$$\begin{aligned} \min_{\Theta} \text{Tr}(\Theta^H \mathbf{T} \Theta \mathbf{Q}) + \text{Tr}(\Theta^H \mathbf{C}^H) + \text{Tr}(\Theta \mathbf{C}) \quad (41) \\ \text{s. t.} \quad (40), (7c). \end{aligned}$$

After invoking some further matrix operations [48], and by defining  $\theta = (\Theta_{1,1}, \Theta_{2,2}, \dots, \Theta_{N,N})^T$ ,  $\Omega \triangleq \mathbf{T} \odot \mathbf{Q}^T$  and  $\mathbf{c} = (\mathbf{C}_{1,1}, \mathbf{C}_{2,2}, \dots, \mathbf{C}_{N,N})^T$ , we arrive at  $\text{Tr}(\Theta^H \mathbf{T} \Theta \mathbf{Q}) \triangleq \theta^H \Omega \theta$ ,  $\text{Tr}(\Theta^H \mathbf{C}^H) = \theta^H \mathbf{c}^*$  and  $\text{Tr}(\Theta \mathbf{C}) = \mathbf{c}^T \theta$ . Similarly, the set of constraints (40) are equivalent to

$$\theta^H \bar{\mathbf{J}}_k \theta + 2\Re\{\theta^H \lambda_k^*\} \geq \ddot{\mathbf{e}}_k, \forall k, \quad (42)$$

where  $\lambda_k = ([\Lambda_k]_{1,1}, [\Lambda_k]_{2,2}, \dots, [\Lambda_k]_{N,N})^T$  and  $\bar{\mathbf{J}}_k = \mathbf{J}_k \odot \mathbf{Q}^T$ . It can be checked that  $\bar{\mathbf{J}}_k, \forall k$  and  $\Omega$  are semi-definite matrices. As for constraint (7c), which can be written as

$$|\theta_n| = \frac{1}{\alpha}, \forall n. \quad (43)$$

Then, we arrive at

$$\begin{aligned} \min_{\theta} f_7(\theta) \triangleq \theta^H \Omega \theta + 2\Re\{\theta^H \mathbf{c}^*\} \quad (44) \\ \text{s. t.} \quad (42), (43). \end{aligned}$$

In  $q$ -th sub-iterations for updating PRB, similar to the operation in (23), we can approximate (42) to its first-order Taylor expansion, which leads to  $\theta^H \bar{\mathbf{J}}_k \theta \geq -(\theta^{(q)})^H \bar{\mathbf{J}}_k \theta^{(q)} + 2\Re\{\theta^H \bar{\mathbf{J}}_k \theta^{(q)}\}$ . Hence, we have

$$2\Re\{\theta^H (\lambda_k^* + \bar{\mathbf{J}}_k \theta^{(q)})\} \geq \ddot{\mathbf{e}}_k + (\theta^{(q)})^H \bar{\mathbf{J}}_k \theta^{(q)} \triangleq \hat{\mathbf{e}}_k^{(q)}. \quad (45)$$

Therefore, the problem becomes

$$\begin{aligned} \min_{\theta} f_7(\theta) \quad (46) \\ \text{s. t.} \quad (43), (45). \end{aligned}$$

Although the objective function  $f_7(\theta)$  is convex and the constraint (45) is linear, Problem 46 is still a non-convex QP problem due to the constant modulus constraints in (43).

Here, we handle the above problem based on the well-known MM approach to obtain optimal PRB in a nearly closed-form with low complexity. The key to the success of MM algorithm lies in constructing a sequence of convex surrogate functions as the bound of  $f_7(\theta)$  in Problem 46. As a benefit, we design the surrogate function by employing the second-order Taylor expansion, which can replace  $\Omega$  by desired structures (e.g., diagonal matrix). Hence, we have the following inequality

$$\begin{aligned} \theta^H \Omega \theta \leq \theta^H \Xi \theta - 2\Re\{\theta^H (\Xi - \Omega) \theta^{(q)}\} \\ + (\theta^{(q)})^H (\Xi - \Omega) \theta^{(q)}, \quad (47) \end{aligned}$$

where  $\Xi = \omega_{\max} \mathbf{I}_N$  with  $\omega_{\max}$  denotes the maximum eigenvalue of  $\Omega$ . Clearly, the inequality (47) holds when  $\Xi \succeq \Omega$  and the equality is achieved at  $\theta = \theta^{(q)}$ . Hence, we arrive that

$$g\left(\theta|\theta^{(q)}\right) = \theta^H \Xi \theta + 2\Re\left\{\theta^H\left(\Omega\theta^{(q)} - \Xi\theta^{(q)} + \mathbf{c}^*\right)\right\} + \left(\theta^{(q)}\right)^H (\Xi - \Omega)\theta^{(q)}. \quad (48)$$

Clearly,  $g\left(\theta|\theta^{(q)}\right)$  satisfies the following conditions: (a)  $g\left(\theta|\theta^{(q)}\right)$  is an upper-bounded function of  $f_7(\theta)$ ; (b)  $g\left(\theta|\theta^{(q)}\right)$  and  $f_7(\theta)$  have the same solution when  $\theta = \theta^{(q)}$ ; (c)  $g\left(\theta|\theta^{(q)}\right)$  and  $f_7(\theta)$  achieve a same gradient at  $\theta^{(q)}$ . The proof can be obtained by employing Example 13 in [26]. Since  $\theta^H \theta = \frac{N}{\alpha}$  holds, we have  $\theta^H \Xi \theta = \frac{N\omega_{\max}}{\alpha}$ , which is a constant with respect to  $\theta$ .

Therefore, by defining  $\mathbf{r}^{(q)} = (\omega_{\max} \mathbf{I}_N - \Omega)\theta^{(q)} - \mathbf{c}^*$  and omitting the irrelevant constant terms with respect to  $\theta$ , i.e.,  $(\theta^{(q)})^H (\Xi - \Omega)\theta^{(q)}$  and  $\theta^H \Xi \theta$ , we have the following problem

$$\begin{aligned} \max_{\theta} \quad & 2\Re\left\{\theta^H \mathbf{r}^{(q)}\right\} \\ \text{s. t.} \quad & (43), (45). \end{aligned} \quad (49)$$

However, due to the non-convex constant modulus constraints in (43), the dual gap is not guaranteed to be zero, and the Lagrangian dual method cannot be used directly. In following, we provide a penalty-based method. It is worth noting that there always exists a vector  $\chi = [\chi_1, \chi_2, \dots, \chi_K]$ , each element of which satisfies  $\chi_k \geq 0$ , and Problem 49 can be reformulated as

$$\begin{aligned} \max_{\theta} \quad & 2\Re\left\{\theta^H \mathbf{r}^{(q)}\right\} + 2\sum_{k=1}^K \chi_k \Re\left\{\theta^H\left(\lambda_k^* + \bar{\mathbf{J}}_k \theta^{(q)}\right)\right\} \\ \text{s. t.} \quad & (43). \end{aligned} \quad (50)$$

It can be checked that Problem 49 and 50 are equivalent, and have the same optimal solution. Interestingly, the objective function and the constraints in Problem 50 are separable with respect to  $\theta_n, \forall n$ . Therefore, we can solve Problem 50 by solving  $N$  separate problems in parallel. Let  $\mathbf{f}^{(q)} = r^{(q)} + \sum_{k=1}^K \chi_k (\lambda_k^* + \bar{\mathbf{J}}_k \theta^{(q)})$ , clearly, Problem 50 can be further rewritten as

$$\max_{\arg \theta_n} \cos\left(\arg \theta_n - \arg \mathbf{f}_n^{(q)}\right), \forall n. \quad (51)$$

Problem 51 is maximized when the phases of  $\theta_n$  and  $\mathbf{f}_n^{(q)}$  are equal. Therefore, the optimal solution of Problem 51 can be sequentially obtained as following

$$\arg \theta_n^{(q+1)} = \arg \mathbf{f}_n^{(q)}, \forall n. \quad (52)$$

Meanwhile, the penalty parameter of  $\chi^{(q+1)}$  can be updated by using the ellipsoid method [49].

The details of optimizing PRB is summarized in Algorithm 2. It can be verified that the sequence of the solutions generated by Algorithm 2, i.e.,  $\{\theta^{(q)}, q = 1, 2, \dots, \hat{q}\}$ , are the optimal solutions of Problem 49, where  $\hat{q}$  represents the maximum number of iterations when algorithm converges. Consequently, we have the following lemma

---

### Algorithm 2 Penalty-based MM/SCA Algorithm for Optimizing PRB

---

**Input:**  $\theta^{(t)}$ , threshold  $\varepsilon_2$ .

**Output:** Optimal value of  $\theta^{(t+1)}$

- 1: **Set**  $\theta^{(0)} \triangleq \theta^{(t)}$ ;
  - 2: **Calculate**  $f_7(\theta^{(0)}) = (\theta^{(0)})^H \Omega \theta^{(0)} + 2\Re\left\{(\theta^{(0)})^H \mathbf{c}^*\right\}$ ;
  - 3: **for**  $q = 1$  to  $2, 3, \dots, q_{\max}$  **do**
  - 4:   **Update**  $\hat{\mathbf{e}}_k^{(q)} = \ddot{\mathbf{e}}_k^{(q)} + (\theta^{(q)})^H \bar{\mathbf{J}}_k \theta^{(q)}$ , by using (45);
  - 5:   **Update**  $\theta^{(q+1)}$ , by using (52);
  - 6:   **if**  $|f_7(\theta^{(q+1)}) - f_7(\theta^{(q)})|/f_7(\theta^{(q)}) < \varepsilon_2$  **then**
  - 6:     **Break** ;
  - 7:   **end if**
  - 8: **end for**
  - 9:  $\theta^{(t+1)} \triangleq \theta^{(\hat{q})}$ .
- 

**Lemma 4.** *The final converged solution of Algorithm 2, i.e.,  $\theta^{(\hat{q})}$ , satisfies the KKT conditions of Problem 44.*

*Proof.* The proof is presented in Appendix A-D.  $\square$

### D. Convergence and Complexity of the Overall Algorithm

The details of the proposed AO-based joint PS ratios, ATB and PRB optimization (JPSAPBO) algorithm are provided in Algorithm 3. The proposed algorithm is guaranteed to converge. Particularly, based on the fact of LDT and FPT methods, we have

$$\begin{aligned} \mathcal{R}(\rho, \mathbf{W}, \Theta) &= f_1(\rho, \mathbf{W}, \Theta, \mathbf{U}) \\ &= f_3(\rho, \mathbf{W}, \Theta, \mathbf{U}, \mathbf{L}). \end{aligned} \quad (53)$$

In  $t$ -th iteration, we have the following inequalities

$$\begin{aligned} & f_3\left(\rho^{(t)}, \mathbf{W}^{(t)}, \Theta^{(t)}, \mathbf{U}^{(t)}, \mathbf{L}^{(t)}\right) \\ & \stackrel{(a)}{\leq} f_3\left(\rho^{(t)}, \mathbf{W}^{(t)}, \Theta^{(t)}, \mathbf{U}^{(t+1)}, \mathbf{L}^{(t)}\right) \\ & \triangleq f_4\left(\rho^{(t)}, \mathbf{W}^{(t)}, \Theta^{(t)}, \mathbf{L}^{(t)}\right) + \text{Const}(\bar{\mathbf{U}}) \\ & \stackrel{(b)}{\leq} f_4\left(\rho^{(t+1)}, \mathbf{W}^{(t)}, \Theta^{(t)}, \mathbf{L}^{(t)}\right) + \text{Const}(\bar{\mathbf{U}}) \\ & \stackrel{(c)}{\leq} f_4\left(\rho^{(t+1)}, \mathbf{W}^{(t)}, \Theta^{(t)}, \mathbf{L}^{(t+1)}\right) + \text{Const}(\bar{\mathbf{U}}) \\ & \triangleq -f_5\left(\mathbf{W}^{(t)}\right) + \text{Const}(\rho, \mathbf{L}, \bar{\mathbf{U}}) \\ & \stackrel{(d)}{\leq} -f_5\left(\mathbf{W}^{(t+1)}\right) + \text{Const}(\rho, \mathbf{L}, \bar{\mathbf{U}}). \end{aligned} \quad (54)$$

where the inequalities, e.g., (a) holds based on the fact that the optimality of  $\mathbf{U}^{(t+1)}$  has been proved in (13) when the other variables are fixed. Similarly, the inequalities of (b) and (c) for optimizing  $\rho$  and  $\mathbf{L}$ , respectively, can also be verified. The inequality (d) holds by employing Algorithm 1.

Moreover, based on the conditions of MM approach, we know that  $g(\theta^{(t+1)}|\theta^{(t)}) \leq g(\theta^{(t)}|\theta^{(t)})$ ,  $g(\theta^{(t)}|\theta^{(t)}) =$

---

**Algorithm 3** AO-based JPSAPBO Algorithm
 

---

**Input:**  $\rho_k^{(1)}, \forall k, \mathbf{W}_k^{(1)}, \forall k, \Theta^{(1)}$ ; threshold  $\varepsilon$ .  
**Output:** Optimal value of  $\rho_k^{\text{opt}}, \mathbf{W}_k^{\text{opt}}, \forall k; \Theta^{\text{opt}}$ .

- 1: **Calculate**  $\Gamma_k^{(1)}, \forall k$ ;
- 2: **Calculate**  $\mathcal{R}^{(1)}(\rho^{(1)}, \mathbf{W}^{(1)}, \Theta^{(1)})$ ;
- 3: **for**  $t = 1$  to  $2, 3, \dots, t_{\max}$  **do**
- 4:   **Update**  $\mathbf{U}_k^{(t+1)}, \forall k$ , by using (14);
- 5:   **Update**  $\rho_k^{(t+1)}, \forall k$ , by using (17);
- 6:   **Update**  $\mathbf{L}_k^{(t+1)}, \forall k$ , by using (19);
- 7:   **Update**  $\mathbf{W}_k^{(t+1)}, \forall k$ , by employing Algorithm 1;
- 8:   **Update**  $\Theta^{(t+1)}$ , by employing Algorithm 2;
- 9:   **if**  $\frac{|\mathcal{R}^{(t+1)}(\rho, \mathbf{W}, \Theta) - \mathcal{R}^{(t)}(\rho, \mathbf{W}, \Theta)|}{\mathcal{R}^{(t)}(\rho, \mathbf{W}, \Theta)} < \varepsilon_3$  **then**
- 9:     Break ;
- 10:   **end if**
- 11: **end for**
- 12:  $\rho_k^{\text{opt}} \triangleq \rho_k^{(\hat{t})}, \mathbf{W}_k^{\text{opt}} \triangleq \mathbf{W}_k^{(\hat{t})}, \forall k; \Theta^{\text{opt}} \triangleq \Theta^{(\hat{t})}$ .

---

$f_7(\theta^{(t)})$ ,  $g(\theta^{(t+1)}|\theta^{(t)}) \geq f_7(\theta^{(t+1)})$ , and  $f_7(\theta^{(t+1)}) \leq f_7(\theta^{(t)})$ . Hence, we have the following inequality

$$\begin{aligned}
 & f_3\left(\rho^{(t+1)}, \mathbf{W}^{(t+1)}, \Theta^{(t)}, \mathbf{U}^{(t+1)}, \mathbf{L}^{(t+1)}\right) \\
 & \triangleq f_6\left(\Theta^{(t)}\right) + \text{Const}\left(\rho, \mathbf{W}, \bar{\mathbf{U}}, \mathbf{L}\right) \\
 & \triangleq -f_7\left(\theta^{(t)}\right) + \text{Const}\left(\rho, \mathbf{W}, \bar{\mathbf{U}}, \mathbf{L}\right) \\
 & \leq -f_7\left(\theta^{(t+1)}\right) + \text{Const}\left(\rho, \mathbf{W}, \bar{\mathbf{U}}, \mathbf{L}\right). \quad (55)
 \end{aligned}$$

Above inequalities verify that  $\mathcal{R}(\rho, \mathbf{W}, \Theta)$  is monotonically non-decreasing after each updating step. In short, it can be concluded that

$$\begin{aligned}
 \mathcal{R}\left(\rho^{(t+1)}, \mathbf{W}^{(t+1)}, \Theta^{(t+1)}\right) & \geq \mathcal{R}\left(\rho^{(t)}, \mathbf{W}^{(t)}, \Theta^{(t)}\right) \\
 & \geq \dots \geq \mathcal{R}\left(\rho^{(1)}, \mathbf{W}^{(1)}, \Theta^{(1)}\right). \quad (56)
 \end{aligned}$$

The inequality in (56) investigate that  $\mathcal{R}(\rho, \mathbf{W}, \Theta)$  is monotonically non-decreasing over iterations. In addition, because of the constraints in (7a)-(7d), the data rate  $\mathcal{R}(\rho, \mathbf{W}, \Theta)$  has an upper bound. As the number of iterations increases, we have  $\mathcal{R}\left(\rho^{(\hat{t})}, \mathbf{W}^{(\hat{t})}, \Theta^{(\hat{t})}\right) \triangleq \mathcal{R}\left(\rho^{\text{opt}}, \mathbf{W}^{\text{opt}}, \Theta^{\text{opt}}\right)$ , where  $\hat{t}$  denotes the maximum number of iterations when Algorithm 3 converges. Therefore, we complete the proof of the strict convergence of Algorithm 3.

Meanwhile, the complexity analysis of Algorithm 3 is given as below. In step 4-6, the complexities of updating  $\mathbf{U}_k$ ,  $\rho_k$  and  $\mathbf{L}_k$  are  $\mathcal{O}(M_u^3)$ ,  $\forall k$ , respectively. In step 7, the complexity of calculating  $\mathbf{W}_k$ ,  $\forall k$  by employing Algorithm 1 is  $\mathcal{O}(\mathcal{I}_1 M_b^3)$ , where  $\mathcal{I}_1$  denotes the number of sub-iterations when Algorithm 1 converges. In step 8, the complexity of calculating the maximum eigenvalue of  $\Omega$  is  $\mathcal{O}(N^3)$  and the complexity of updating  $\theta$  is  $\mathcal{O}(\mathcal{I}_2 N^2)$ , where  $\mathcal{I}_2$  stands for the number of sub-iterations when Algorithm 2 converges. Therefore, the total complexity of Algorithm 3 is  $\mathcal{O}(\mathcal{I}_{\text{total}}(K(3M_u^3 + \mathcal{I}_1 M_b^3) + \mathcal{I}_2 N^2 + N^3))$ , where  $\mathcal{I}_{\text{total}}$  is the number of iterations when Algorithm 3 converges.

TABLE I  
SIMULATION PARAMETERS

Parameters	Values
Cell coverage	5 m
AP location	(0 m, 0 m)
IRS location	(5 m, 5 m)
Center of PSRs location	(5 m, 0 m)
Number of antennas of the AP	$M_b = 8$
Number of antennas of each PSR	$M_u = 2$
Number of PSRs	$K = 4$
Number of reflective elements	$N = 30$
Path loss at the reference distance	$C_0 = -30$ dB
The maximum transmission power	$P_{\max} = 10$ W
Path loss exponent of direct channel	$\chi_{\text{direct}} = 3.6$
Path loss exponent of IRS-related channel	$\chi_{\text{relate}} = 2.2$
Rician factor of channels	$\beta = 5$ dB
Antenna noise power	$\sigma_k^2 = \sigma^2 = -50$ dBm
Signal Processing noise power	$\delta_k^2 = \delta^2 = -40$ dBm
Minimum harvested power requirement	$\bar{\mathbf{e}}_k = \bar{\mathbf{e}} = 0.5$ mW
Energy conversion efficiency	$\eta_k = \eta = 0.7$
Threshold	$\varepsilon_{1,2,3} = 10^{-6}$

#### IV. NUMERICAL SIMULATION RESULTS

In this section, numerical simulation results are provided to evaluate the performance of the proposed AO-based JPSAPBO algorithm. It is assumed that there is a uniform linear array (ULA) at the AP side, and there is a uniform rectangular array (URA) at the IRS side. The total number of reflective elements of the IRS is assumed to be  $N = N_x N_y$ , where  $N_h$  and  $N_v$  denote the numbers of reflecting elements along horizon and vertical, respectively. Since the AP, the IRS and the PSRs are closed to each other, the small-scale channel fading is assumed to be Rician fading, and the channels, i.e., the AP-IRS channel, the AP-PSRs channels and the IRS-PSRs channels can be mathematically modeled as

$$\hat{\mathbf{H}}_i = \sqrt{\frac{\beta_i}{\beta_i + 1}} \hat{\mathbf{H}}_i^{\text{LOS}} + \sqrt{\frac{1}{\beta_i + 1}} \hat{\mathbf{H}}_i^{\text{NLOS}}, \quad (57)$$

where  $\beta_i$  stands for the Rician factor, and  $\hat{\mathbf{H}}_i^{\text{LOS}}$  is the deterministic line of sight (LOS),  $\hat{\mathbf{H}}_i^{\text{NLOS}}$  is the non-line-of-sight (NLOS) component, which follow Rayleigh fading model, with  $i \in \{\text{AP-IRS}, \text{AP-PSRs}, \text{IRS-PSRs}\}$ . Meanwhile, the distance-dependent large-scale path loss is given as

$$\mathcal{L}(d) = C_0 \left(\frac{d}{D_0}\right)^{-\chi_j}, \quad (58)$$

where  $C_0$  corresponds to the path loss at the reference distance of  $D_0 = 1\text{m}$ ,  $d$  is the link distance and  $\chi_j$  denotes path loss exponent, where  $j \in \{\text{direct}, \text{relate}\}$ . The other simulation parameters are summarized in Table I, unless otherwise stated.

Before the performance comparison, we first study the convergence behavior of the proposed AO-based JPSAPBO algorithm in Fig. 3. Particularly, we plot the data rate versus the number of iterations for the various number of reflective elements, i.e.,  $N = 10$ ,  $N = 30$  and  $N = 50$ . The curves are consistent to our expectation, as we can observe that the proposed AO-based JPSAPBO algorithm converges to a stationary point after a few iterations. Besides, another observation is that more reflective elements only leads to a slightly slower convergence speed, e.g., for a large-scale IRS

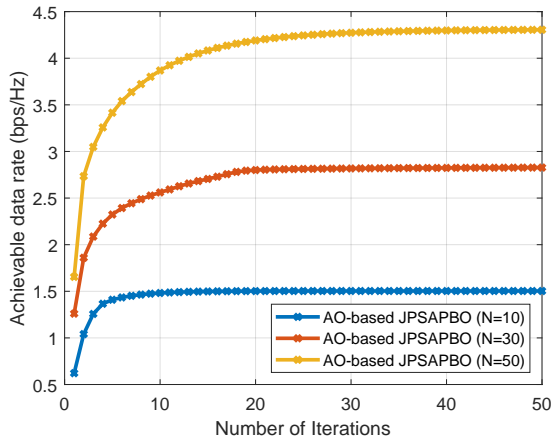


Fig. 3. Convergence behavior of the AO-based JPSAPBO algorithm under different number of reflective elements.

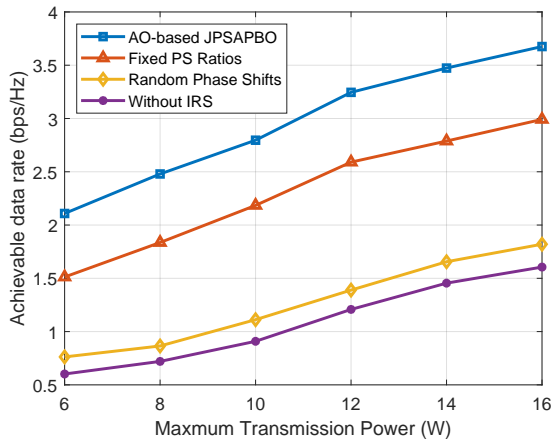


Fig. 4. Achievable data rate versus the maximum transmission power of the AP, i.e.,  $P_{\max}$ .

with  $N = 50$ , the proposed AO-based JPSAPBO algorithm can also converge in 30 iterations.

Then, in the following, we study the performance gain achieved by the proposed AO-based JPSAPBO algorithm. For comparison, we introduce three benchmark system design schemes to validate the performance as following

- Fixed PS ratios: In this scheme, the PS ratios of PSRs are fixed (i.e.,  $\rho_k = 0.5, \forall k$ ) and without optimized, while the ATB and PRB are need to be optimized;
- Random Phase Shifts: In this scheme, the phase shifts of IRS elements are random, and only the PS ratios at the PSRs side and ATB at the AP side need to be optimized;
- Without IRS: In this scheme, there is no IRS in the system, i.e., it is a conventional SWIPT, and only two sides, i.e., the AP side and the PSRs side need to be optimized.

As shown in Fig. 4, we investigate the data rate versus the maximum transmission power of AP, i.e.,  $P_{\max}$  for different schemes. The proposed AO-based JPSAPBO algorithm achieves a significant performance gain comparing with benchmark schemes. Meanwhile, it can be seen that the performance

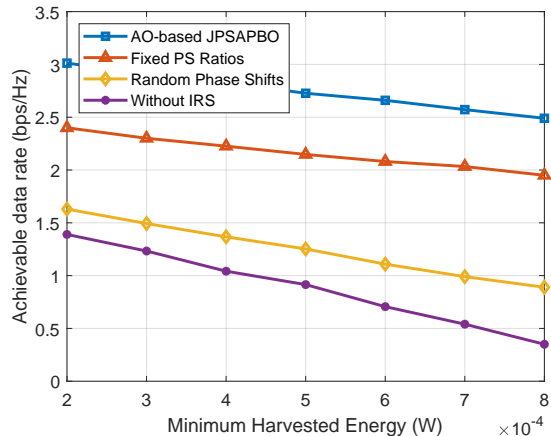


Fig. 5. Achievable data rate versus the minimum harvested energy requirement of PSRs, i.e.,  $\bar{e}_k, \forall k$ .

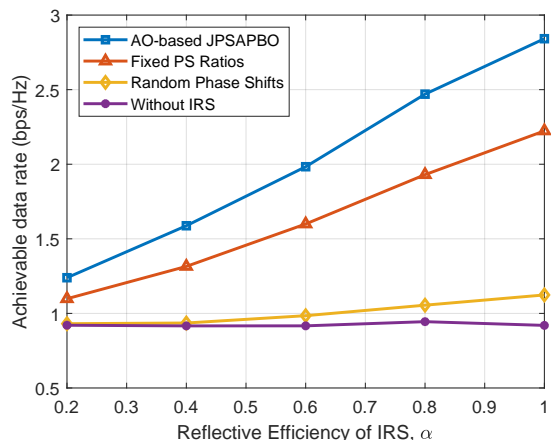


Fig. 6. Achievable data rate versus the reflective efficiency of IRS, i.e.,  $\alpha$ .

achieved by the Fixed PS ratios scheme is better than both the Random Phase Shifts scheme and the Without IRS scheme, this implies that IRS can enhance the performance of SWIPT system, and PRB of IRS need be carefully optimized to achieved a higher data rate.

As shown in Fig. 5 illustrates the data rate achieved by the proposed AO-based JPSAPBO algorithm and benchmark schemes over the minimum harvested power requirement of PSRs, i.e.,  $\bar{e}_k, \forall k$ . As we can see, the proposed AO-based JPSAPBO algorithm in this paper outperforms the benchmarks significantly. In addition, with the increased minimum harvested energy, the gap between the IRS-related schemes and the Without IRS scheme becomes larger, and this indicates that the systems with IRS are more robust against the minimum harvest energy comparing with the system without IRS.

As shown in Fig. 6, we study the achievable data rate versus the reflective efficiency of IRS, i.e.,  $\alpha$ . As we can see from the figure, for all IRS reflective efficiencies, the proposed AO-based JPSAPBO algorithm outperforms other benchmarks considerably. Additionally, the Fixed PS Ratios scheme also achieves a better performance gain than both the Random Phase Shifts and the Without IRS schemes. Finally, for the

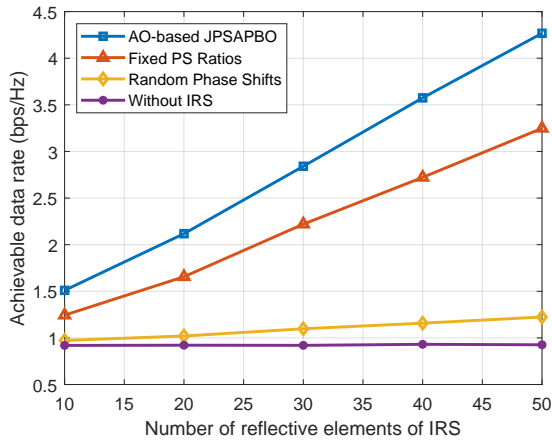


Fig. 7. Achievable data rate versus the number of reflective elements of IRS, i.e.,  $N$ .

large reflective efficiency of IRS, i.e.,  $\alpha \geq 0.4$ , the Random Phase Shifts scheme achieves a higher data rate compares with the Without IRS scheme, and this implies that the IRS can enhance the performance of the SWIPT system.

As shown in Fig. 7, we study that the achievable data rate versus the number of reflective elements of IRS, i.e.,  $N$ . It can be observed that by increasing the number of reflective elements of IRS, the data rate achieved by all schemes except for Without IRS scheme increases monotonically as well, and the proposed AO-based JPSAPBO algorithm outperforms other three benchmarks significantly. In addition, the Fixed PS ratios scheme significantly outperforms both the Random Phase Shifts and the Without IRS schemes, especially for large value of reflective elements, which is due to the fact that PRB of IRS has been carefully optimized. Finally, the Random Phase Shifts scheme also achieves a higher rate than the Without IRS scheme, especially for large number of elements, and this implies that IRS leads to a significant performance gain, even though PRB of IRS has not been optimized.

## V. CONCLUSION

In this paper, we investigated the achievable data rate maximization problem in the IRS-assisted SWIPT system with multiple integrated PSRs, which can perform both ID and EH. To address this unsolved problem, we proposed a joint optimization framework. Particularly, we decoupled the problem and decomposed it into several sub-problems. Then, we proposed the AO-based JPSAPBO algorithm to solve the sub-problems in an AO manner, and obtain the optimal solutions in nearly closed-forms iteratively. Simulation results indicated that the proposed AO-based JPSAPBO algorithm achieved a substantial performance gain and the IRS can significantly enhance the performance.

### APPENDIX A PROOF OF LEMMA

#### A. Proof of Lemma 1

Clearly, Problem 16 is equivalent to Problem 8 with respect to  $\rho$ , and  $\rho$  only exists in the last term of  $f_1$ . Therefore,

we recast  $f_1$  as  $f_1(\rho, \mathbf{W}^{(t)}, \Theta^{(t)}, \bar{\mathbf{U}}^{(t+1)}) \triangleq \text{Tr}(\mathcal{F}(\rho)) + \text{Const}(\bar{\mathbf{U}})$ , and where

$$\mathcal{F}(\rho) \triangleq \sum_{k=1}^K \frac{\mathcal{A}_k}{\mathcal{B}_k + \frac{\mathcal{C}_k}{\rho_k}}, \quad (59)$$

where  $\mathcal{A}_k \triangleq \bar{\mathbf{U}}_k \mathbf{H}_k^H \mathbf{W}_k \mathbf{W}_k^H \mathbf{H}_k$ ,  $\mathcal{B}_k \triangleq \sum_{i=1}^K \mathbf{H}_i^H \mathbf{W}_i \mathbf{W}_i^H \mathbf{H}_k + \sigma_k^2 \mathbf{I}_{M_u}$  and  $\mathcal{C}_k \triangleq \delta_k^2 \mathbf{I}_{M_u}$ . Since the PS ratio of each PSR is independent, the second-order derivative of  $\mathcal{F}(\rho)$  as  $\frac{\partial^2 \mathcal{F}(\rho)}{\partial \rho_i \partial \rho_j} = 0, \forall i \neq j$  holds. Therefore, the Hessian matrix of  $\mathcal{F}(\rho)$  can be expressed as

$$\frac{\partial^2 \mathcal{F}(\rho)}{\partial \rho^2} = \text{diag} \left\{ \frac{\partial^2 \mathcal{F}(\rho)}{\partial \rho_1^2}, \frac{\partial^2 \mathcal{F}(\rho)}{\partial \rho_2^2}, \dots, \frac{\partial^2 \mathcal{F}(\rho)}{\partial \rho_K^2} \right\}, \quad (60)$$

each element of the diagonal matrix is determined as

$$\frac{\partial^2 \mathcal{F}(\rho)}{\partial \rho_k^2} = \frac{-2\mathcal{A}_k \mathcal{B}_k \mathcal{C}_k}{(\mathcal{B}_k \rho_k + \mathcal{C}_k)^3}, \quad \forall k. \quad (61)$$

It is clear that  $\mathcal{A}_k \geq 0$ ,  $\mathcal{B}_k \geq 0$  and  $\mathcal{C}_k \geq 0, \forall k$  are hold. Therefore,  $\frac{\partial^2 \mathcal{F}(\rho)}{\partial \rho_k^2} < 0$  is always satisfying, which leads to that  $\mathcal{F}(\rho)$  is a concave function on  $\rho$ . Moreover, we have the first-order derivative of  $\mathcal{F}(\rho)$  as  $\frac{\partial \mathcal{F}(\rho)}{\partial \rho_k} = \frac{\mathcal{A}_k \mathcal{C}_k}{(\rho_k \mathcal{B}_k + \mathcal{C}_k)^2} > 0, \forall k$ . Therefore,  $\mathcal{F}(\rho)$  is a monotonous increasing function. Similarly, it can be readily verified that the objective function of Problem 16 is also concave and monotonously increasing on  $\rho$ . The proof of the lemma is completed.

#### B. Proof of Lemma 2

Clearly, the value of  $\rho_k, \forall k$  should be bounded by  $\rho_k^{\min} \leq \rho_k \leq \rho_k^{\max}$ , where  $\rho_k^{\min} > 0$  ensures for satisfying the minimum value of PS ratio in constraint (7d), and  $\rho_k^{\max} = 1 - \frac{\bar{\epsilon}_k}{\eta_k \text{Tr}(\sum_{i=1}^K \mathbf{H}_i^H \mathbf{W}_i \mathbf{W}_i^H \mathbf{H}_k)}$  ensures the harvested energy is larger than the minimum EH requirement in constraint (7b). Moreover, according to Lemma 1, we know the objective function is monotonous increasing with respect to  $\rho$ , hence we have

$$\rho_k^{(t+1)} \triangleq \max \left\{ \rho_k^{\text{low}} \triangleq \max \{0, \rho_k^{\min}\}, \rho_k^{\text{up}} \triangleq \min \{\rho_k^{\max}, 1\} \right\}. \quad (62)$$

Since  $\frac{\bar{\epsilon}_k}{\eta_k \text{Tr}(\sum_{i=1}^K \mathbf{H}_i^H \mathbf{W}_i \mathbf{W}_i^H \mathbf{H}_k)} > 0$  holds, we have  $\rho_k^{\text{up}} = \rho_k^{\max}, \forall k$ . Therefore, when  $\rho_k^{\text{up}} > \rho_k^{\text{low}} = 0$ , Problem 16 is feasible. This completes the proof of Lemma 2.

#### C. Proof of Lemma 3

It is clear that the sequence of feasible solutions of ATB  $\{\mathbf{W}^{(n)}, \forall n = 1, 2, \dots, \hat{n}\}$  are the optimal solutions of Problem 25, since they satisfy the KKT conditions of Problem 25. As following, we prove that the converged solution of ATB, i.e.,  $\mathbf{W}^{(\hat{n})}$  also satisfies the KKT conditions of Problem 21. By

defining the corresponding Lagrangian function of Problem 21 as following

$$\begin{aligned} \bar{\mathcal{L}}(\mathbf{W}, \bar{\tau}, \bar{\mu}) &= \sum_{k=1}^K \text{Tr}(\mathbf{W}_k^H \mathbf{A} \mathbf{W}_k) - 2 \sum_{k=1}^K \text{Tr}(\mathbf{W}_k^H \mathbf{S}_k) \\ &+ \bar{\tau} \left( \sum_{k=1}^K \text{Tr}(\mathbf{W}_k^H \mathbf{W}_k) - P_{\max} \right) \\ &- \sum_{k=1}^K \bar{\mu}_k \left( \text{Tr} \left( \sum_{i=1}^K \mathbf{W}_i^H \mathbf{B}_k \mathbf{W}_i \right) - \dot{\mathbf{e}}_k \right). \end{aligned} \quad (63)$$

Therefore, the KKT conditions of Problem 21 can be represented as

$$\begin{aligned} \text{Tr}((\mathbf{A} + \bar{\tau} \mathbf{I}_{M_b}) \mathbf{W}_k - \bar{\mu}_k \mathbf{B}_k \mathbf{W}_k - \mathbf{S}_k) &= 0, \forall k; \\ \bar{\tau} \left( \sum_{k=1}^K \text{Tr}(\mathbf{W}_k^H \mathbf{W}_k) - P_{\max} \right) &= 0; \\ \bar{\mu}_k \left( \text{Tr} \left( \sum_{i=1}^K \mathbf{W}_i^H \mathbf{B}_k \mathbf{W}_i \right) - \dot{\mathbf{e}}_k \right) &= 0, \forall k. \end{aligned} \quad (64)$$

With the converged solution  $\mathbf{W}_k^{(\hat{n})}, \forall k$ , it can be readily checked that there must exist the corresponding Lagrangian multipliers, i.e.,  $\bar{\tau}^{(\hat{n})}$  and  $\bar{\mu}_k^{(\hat{n})}, \forall k$ , for ensuring that the above KKT conditions of Problem 21 are satisfied. Hence, the proof of Lemma 3 is complete.

#### D. Proof of Lemma 4

By denoting  $\bar{\chi}_k \geq 0, \forall k$  and  $\zeta_n \geq 0, \forall n$  as the dual variables associated with the constraints (42) and (43), the Lagrange function of Problem 44 can be expressed as

$$\begin{aligned} \mathcal{L}(\theta, \bar{\chi}, \zeta) &= f_7(\theta) - \sum_{k=1}^K \bar{\chi}_k (\theta^H \bar{\mathbf{J}}_k \theta + 2\Re\{\theta^H \lambda_k^*\} - \ddot{\mathbf{e}}_k) \\ &+ \sum_{n=1}^N \zeta_n \left( |\theta_n| - \frac{1}{\alpha} \right), \end{aligned} \quad (65)$$

and the KKT conditions are given as

$$\begin{aligned} \nabla_{\theta} f_7(\theta) - \sum_{k=1}^K 2\bar{\chi}_k (\theta^H \bar{\mathbf{J}}_k + \lambda_k^*) + \sum_{n=1}^N \zeta_n \nabla_{\theta} (|\theta_n|) &= 0; \\ \sum_{k=1}^K \bar{\chi}_k (\theta^H \bar{\mathbf{J}}_k \theta + 2\Re\{\theta^H \lambda_k^*\} - \ddot{\mathbf{e}}_k) &= 0; \\ \zeta_n \left( |\theta_n| - \frac{1}{\alpha} \right) &= 0, \forall n. \end{aligned} \quad (66)$$

We assume that the final converged solution of Algorithm 2 is  $\theta^{(\hat{q})}$ . According to the properties of SCA approach, the constraints (42) and (45) have the same gradient value at point  $\theta = \theta^{(\hat{q})}$ . Meanwhile, according to the properties of MM approach, the same gradient of functions  $f_7(\theta)$  and  $g(\theta|\theta^{(\hat{q})})$  achieved at point  $\theta^{(\hat{q})}$ . Additional, the constant modulus constraint is ensured by employing the updating rule in (52). Therefore, with the final converged solution of Algorithm 2, i.e.,  $\theta^{(\hat{q})}$ , there must exist the corresponding multipliers  $\bar{\chi}^{(\hat{q})}$  and  $\zeta^{(\hat{q})}$  for guaranteeing that the KKT conditions of Problem 44 are satisfied. The proof is completed.

## APPENDIX B CONNECTION WITH MMSE RECEIVER

We consider the MMSE matrix of each PSR denoted by  $\hat{\mathbf{L}}_k, \forall k$ , and the decoded signal can be wittered as

$$\begin{aligned} \hat{\mathbf{s}}_k &= \frac{1}{\sqrt{\rho_k}} \hat{\mathbf{L}}_k^H \mathbf{y}_k^{\text{ID}} \\ &= \hat{\mathbf{L}}_k^H \sum_{i=1}^K \mathbf{H}_k \mathbf{W}_i \mathbf{s}_i + \hat{\mathbf{L}}_k^H \mathbf{n}_k + \frac{1}{\sqrt{\rho_k}} \hat{\mathbf{L}}_k^H \mathbf{z}_k, \forall k. \end{aligned} \quad (67)$$

Consequently, the MSE can be expressed as

$$\begin{aligned} \text{MSE}_k &= \mathbb{E} \left\{ (\hat{\mathbf{s}}_k - \mathbf{s}_k) (\hat{\mathbf{s}}_k - \mathbf{s}_k)^H \right\} \\ &= \mathbf{I}_{M_u} + \sum_{i=1}^K \hat{\mathbf{L}}_k^H \mathbf{H}_k^H \mathbf{W}_i \mathbf{W}_i^H \mathbf{H}_k \hat{\mathbf{L}}_k - \hat{\mathbf{L}}_k^H \mathbf{H}_k^H \mathbf{W}_k \\ &- \mathbf{W}_k^H \mathbf{H}_k \hat{\mathbf{L}}_k + \hat{\mathbf{L}}_k^H \left( \sigma_k^2 + \frac{\delta_k^2}{\rho_k} \right) \hat{\mathbf{L}}_k, \forall k. \end{aligned} \quad (68)$$

Since the maximum transmission power at AP and the minimum EH requirement constraints of PSRs are independent of ID operation, and with fixed ATB and PS ratios, the sub-problem for solving the decoding matrix is given as

$$\min_{\hat{\mathbf{L}}_k} \text{MSE}_k, \forall k. \quad (69)$$

The closed-form solution of above problem is

$$\hat{\mathbf{L}}_k = \frac{\mathbf{H}_k^H \mathbf{W}_k}{\sum_{i=1}^K \mathbf{H}_k^H \mathbf{W}_i \mathbf{W}_i^H \mathbf{H}_k + \sigma_k^2 \mathbf{I}_{M_u} + \delta_k^2 / \rho_k \mathbf{I}_{M_u}}, \forall k. \quad (70)$$

As aforementioned, this appendix implies that there is a connection between the FPT and the MMSE matrices. In fact, MMSE decoding matrix can be interpreted as a special form of the FPT receiver. For details, please refer to [21]–[23].

## REFERENCES

- [1] Gang Yang, Dongdong Yuan, Ying-Chang Liang, Rui Zhang, and Victor C. M. Leung. Optimal resource allocation in full-duplex ambient backscatter communication networks for wireless-powered iot. *IEEE Internet of Things Journal*, 6(2):2612–2625, 2019.
- [2] Qingdong Yue, Jie Hu, Kun Yang, and Chuan Huang. Transceiver design for simultaneous wireless information and power multicast in multi-user mmwave mimo system. *IEEE Transactions on Vehicular Technology*, 69(10):11394–11407, 2020.
- [3] Ioannis Krikidis, Stelios Timotheou, Symeon Nikolaou, Gan Zheng, Derrick Wing Kwan Ng, and Robert Schober. Simultaneous wireless information and power transfer in modern communication systems. *IEEE Communications Magazine*, 52(11):104–110, 2014.
- [4] Tharindu D. Ponnimbaduge Perera, Dushantha Nalin K. Jayakody, Shree Krishna Sharma, Symeon Chatzinotas, and Jun Li. Simultaneous wireless information and power transfer (swipt): Recent advances and future challenges. *IEEE Communications Surveys Tutorials*, 20(1):264–302, 2018.
- [5] J. Hu, Y. Zhao, and K. Yang. Modulation and coding design for simultaneous wireless information and power transfer. *IEEE Communications Magazine*, 57(5):124–130, 2019.
- [6] J. Hu, M. Li, K. Yang, S. X. Ng, and K. Wong. Unary coding controlled simultaneous wireless information and power transfer. *IEEE Transactions on Wireless Communications*, 19(1):637–649, 2020.
- [7] B. Clerckx, R. Zhang, R. Schober, D. W. K. Ng, D. I. Kim, and H. V. Poor. Fundamentals of wireless information and power transfer: From rf energy harvester models to signal and system designs. *IEEE Journal on Selected Areas in Communications*, 37(1):4–33, 2019.

- [8] J. Hu, K. Yang, G. Wen, and L. Hanzo. Integrated data and energy communication network: A comprehensive survey. *IEEE Communications Surveys Tutorials*, 20(4):3169–3219, 2018.
- [9] Q. Shi, W. Xu, T. H. Chang, Y. Wang, and E. Song. Joint beamforming and power splitting for miso interference channel with swipt: An socr relaxation and decentralized algorithm. *IEEE Transactions on Signal Processing*, 62(23):6194–6208, 2014.
- [10] Gang Yang, Chin Keong Ho, Rui Zhang, and Yong Liang Guan. Throughput optimization for massive mimo systems powered by wireless energy transfer. *IEEE Journal on Selected Areas in Communications*, 33(8):1640–1650, 2015.
- [11] Gang Yang, Mohammad R. Vedady Moghadam, and Rui Zhang. Magnetic mimo signal processing and optimization for wireless power transfer. *IEEE Transactions on Signal Processing*, 65(11):2860–2874, 2017.
- [12] Q. Tao, J. Wang, and C. Zhong. Performance analysis of intelligent reflecting surface aided communication systems. *IEEE Communications Letters*, 24(11):2464–2468, 2020.
- [13] M. Di Renzo, A. Zappone, M. Debbah, M. S. Alouini, C. Yuen, J. de Rosny, and S. Tretjakov. Smart radio environments empowered by reconfigurable intelligent surfaces: How it works, state of research, and the road ahead. *IEEE Journal on Selected Areas in Communications*, 38(11):2450–2525, 2020.
- [14] Marco Di Renzo, Merouane Debbah, Dinh-Thuy Phan-Huy, Alessio Zappone, Mohamed-Slim Alouini, Chau Yuen, Vincenzo Sciancalepore, George C Alexandropoulos, Jakob Hoydis, Haris Gacanin, et al. Smart radio environments empowered by reconfigurable ai meta-surfaces: An idea whose time has come. *EURASIP Journal on Wireless Communications and Networking*, 2019(1):1–20, 2019.
- [15] Xiaoling Hu, Caijun Zhong, Yu Zhang, Xiaoming Chen, and Zhaoyang Zhang. Location information aided multiple intelligent reflecting surface systems. *IEEE Transactions on Communications*, 68(12):7948–7962, 2020.
- [16] J. Zhang, Y. Zhang, C. Zhong, and Z. Zhang. Robust design for intelligent reflecting surfaces assisted miso systems. *IEEE Communications Letters*, 24(10):2353–2357, 2020.
- [17] Hong Shen, Wei Xu, Shulei Gong, Chunming Zhao, and Derrick Wing Kwan Ng. Beamforming optimization for irs-aided communications with transceiver hardware impairments. *IEEE Transactions on Communications*, 69(2):1214–1227, 2021.
- [18] Zhiqiang Wei, Yuanxin Cai, Zhuo Sun, Derrick Wing Kwan Ng, Jinhong Yuan, Mingyu Zhou, and Lixin Sun. Sum-rate maximization for irs-assisted uav ofdma communication systems. *IEEE Transactions on Wireless Communications*, 20(4):2530–2550, 2021.
- [19] Yu Zhang, Caijun Zhong, Zhaoyang Zhang, and Weidang Lu. Sum rate optimization for two way communications with intelligent reflecting surface. *IEEE Communications Letters*, 24(5):1090–1094, 2020.
- [20] Huayan Guo, Ying-Chang Liang, Jie Chen, and Erik G. Larsson. Weighted sum-rate maximization for reconfigurable intelligent surface aided wireless networks. *IEEE Transactions on Wireless Communications*, 19(5):3064–3076, 2020.
- [21] Kaiming Shen and Wei Yu. Fractional programming for communication systems—part i: Power control and beamforming. *IEEE Transactions on Signal Processing*, 66(10):2616–2630, 2018.
- [22] Kaiming Shen and Wei Yu. Fractional programming for communication systems—part ii: Uplink scheduling via matching. *IEEE Transactions on Signal Processing*, 66(10):2631–2644, 2018.
- [23] Kaiming Shen, Wei Yu, Licheng Zhao, and Daniel P. Palomar. Optimization of mimo device-to-device networks via matrix fractional programming: A minorization–maximization approach. *IEEE/ACM Transactions on Networking*, 27(5):2164–2177, 2019.
- [24] Zijian Zhang and Linglong Dai. Capacity improvement in wideband reconfigurable intelligent surface-aided cell-free network. In *2020 IEEE 21st International Workshop on Signal Processing Advances in Wireless Communications (SPAWC)*, pages 1–5, 2020.
- [25] Gui Zhou, Cunhua Pan, Hong Ren, Kezhi Wang, and Arumugam Nallanathan. Intelligent reflecting surface aided multigroup multicast miso communication systems. *IEEE Transactions on Signal Processing*, 68:3236–3251, 2020.
- [26] Y. Sun, P. Babu, and D. P. Palomar. Majorization-minimization algorithms in signal processing, communications, and machine learning. *IEEE Transactions on Signal Processing*, 65(3):794–816, 2017.
- [27] C. Pan, H. Ren, K. Wang, W. Xu, M. ElKashlan, A. Nallanathan, and L. Hanzo. Multicell mimo communications relying on intelligent reflecting surfaces. *IEEE Transactions on Wireless Communications*, 19(8):5218–5233, 2020.
- [28] Meng Hua, Qingqing Wu, Derrick Wing Kwan Ng, Jun Zhao, and Luxi Yang. Intelligent reflecting surface-aided joint processing coordinated multipoint transmission. *IEEE Transactions on Communications*, 69(3):1650–1665, 2021.
- [29] Q. Shi, M. Razaviyayn, Z. Luo, and C. He. An iteratively weighted mmse approach to distributed sum-utility maximization for a mimo interfering broadcast channel. *IEEE Transactions on Signal Processing*, 59(9):4331–4340, 2011.
- [30] Zhi-Quan Luo, Wing-Kin Ma, Anthony Man-Cho So, Yinyu Ye, and Shuzhong Zhang. Semidefinite relaxation of quadratic optimization problems. *IEEE Signal Processing Magazine*, 27(3):20–34, 2010.
- [31] H. Shen, W. Xu, S. Gong, Z. He, and C. Zhao. Secrecy rate maximization for intelligent reflecting surface assisted multi-antenna communications. *IEEE Communications Letters*, 23(9):1488–1492, 2019.
- [32] Gang Yang, Xinyue Xu, Ying-Chang Liang, and Marco Di Renzo. Reconfigurable intelligent surface-assisted non-orthogonal multiple access. *IEEE Transactions on Wireless Communications*, 20(5):3137–3151, 2021.
- [33] Gang Yang, Yating Liao, Ying-Chang Liang, and Olav Tirkkonen. Reconfigurable intelligent surface empowered underlying device-to-device communication. In *2021 IEEE Wireless Communications and Networking Conference (WCNC)*, pages 1–6, 2021.
- [34] Jiabao Gao, Caijun Zhong, Xiaoming Chen, Hai Lin, and Zhaoyang Zhang. Unsupervised learning for passive beamforming. *IEEE Communications Letters*, 24(5):1052–1056, 2020.
- [35] Xiaoling Hu, Feifei Gao, Caijun Zhong, Xiaoming Chen, Yu Zhang, and Zhaoyang Zhang. An angle domain design framework for intelligent reflecting surface systems. In *GLOBECOM 2020 - 2020 IEEE Global Communications Conference*, pages 1–6, 2020.
- [36] Gui Zhou, Cunhua Pan, Hong Ren, Kezhi Wang, Arumugam Nallanathan, and Kai-Kit Wong. User cooperation for irs-aided secure swipt mimo: Active attacks and passive eavesdropping. *arXiv preprint arXiv:2006.05347*, 2020.
- [37] Dongfang Xu, Xianghao Yu, Vahid Jamali, Derrick Wing Kwan Ng, and Robert Schober. Resource allocation for large irs-assisted swipt systems with non-linear energy harvesting model. *arXiv preprint arXiv:2010.00846*, 2020.
- [38] Q. Wu and R. Zhang. Weighted sum power maximization for intelligent reflecting surface aided swipt. *IEEE Wireless Communications Letters*, 9(5):586–590, 2020.
- [39] Q. Wu and R. Zhang. Joint active and passive beamforming optimization for intelligent reflecting surface assisted swipt under qos constraints. *IEEE Journal on Selected Areas in Communications*, 38(8):1735–1748, 2020.
- [40] C. Pan, H. Ren, K. Wang, M. ElKashlan, A. Nallanathan, J. Wang, and L. Hanzo. Intelligent reflecting surface aided mimo broadcasting for simultaneous wireless information and power transfer. *IEEE Journal on Selected Areas in Communications*, 38(8):1719–1734, 2020.
- [41] Shayan Zargari, Ata Khalili, and Rui Zhang. Energy efficiency maximization via joint active and passive beamforming design for multiuser miso irs-aided swipt. *IEEE Wireless Communications Letters*, 10(3):557–561, 2021.
- [42] Shayan Zargari, Ata Khalili, Qingqing Wu, Mohammad Robot Mili, and Derrick Wing Kwan Ng. Max-min fair energy-efficient beamforming design for intelligent reflecting surface-aided swipt systems with non-linear energy harvesting model. *IEEE Transactions on Vehicular Technology*, pages 1–1, 2021.
- [43] Wenhui Zhang, Jindan Xu, Wei Xu, Derrick Wing Kwan Ng, and Huan Sun. Cascaded channel estimation for irs-assisted mmwave multi-antenna with quantized beamforming. *IEEE Communications Letters*, 25(2):593–597, 2021.
- [44] J. Tang, J. Luo, J. Ou, X. Zhang, N. Zhao, D. K. C. So, and K. K. Wong. Decoupling or learning: Joint power splitting and allocation in mc-noma with swipt. *IEEE Transactions on Communications*, 68(9):5834–5848, 2020.
- [45] H. Zhang, A. Dong, J. Shi, and D. Yuan. Joint transceiver and power splitting optimization for multiuser mimo swipt under mse qos constraints. *IEEE Transactions on Vehicular Technology*, PP(8):1–1, 2017.
- [46] Michael Grant and Stephen Boyd. CVX: Matlab software for disciplined convex programming, version 2.1. <http://cvxr.com/cvx>, March 2014.
- [47] Org. Cambridge. Ebooks. Online. Book. Author@Af. *Complex-Valued Matrix Derivatives*. Complex-Valued Matrix Derivatives.
- [48] Ben-Tal and Nemirovskii. Lectures on modern convex optimization. 2012.
- [49] S. Boyd and L. Vandenberghe. *Convex Optimization*. Convex Optimization, 2004.